ChemPubSoc Europe

DOI: 10.1002/ejic.201900706

EurJIC European Journal of Inorganic Chemistry

Minireview

Radiometal Complexes

The Use of the Macrocyclic Chelator DOTA in Radiochemical Separations

Zsolt Baranyai,[a] Gyula Tircsó,[b] and Frank Rösch*[c]

Abstract: Radiometals play an important role in the diagnosis of physiological processes in vivo by means of imaging technologies, but also increasingly contribute to the treatment of diseases. The by far dominant way to apply the advantages of nuclear transformations of radiometals is the use of radiometal-ligand complexes. In this context, it turns out that DOTA (and its derivatives) currently is the most potent chelator. This article reviews the physico-chemical properties of DOTA and its [*M(DOTA)]$^{-}$ complexes, which made the DOTA moiety the dominant chelator for theranostics in radiopharmaceutical chemistry and nuclear medicine. Interestingly, and beyond nuclear medicine applications, the physico-chemical properties of [*M(DOTA)] complexes open access to unique radiochemical separation strategies, which for decades appeared to be impossible not only within conventional chemistry, but also within modern radiochemistry. We will discuss three groups of such separations: *i*) the radiochemical separation of two chemically very similar elements such as two neighbor lanthanides, *ii*) the radiochemical separation of two isotopes of the same element, and even *iii*) the radiochemical separation of two nuclear levels of one and the same isotope.

1. Introduction

Radiometals play an important role in the diagnosis of physiological processes in vivo by means of imaging technologies, but increasingly contribute also to the treatment of diseases. Only in very few cases, the radiometals are applied as cations: ^{82}Rb and ^{201}Tl for myocardial imaging, ^{89}Sr and ^{223}Ra for treatment of bone metastases. The by far dominant way, however, is the use of radiometal-ligand complexes. Despite the many ligands developed for the rich coordination chemistry of the many valency states of technetium (and rhenium), most of the trivalent, but also some divalent and tetravalent radiometals utilize polyamino-polycarboxylate ligands to coordinate the central metal cation.

Because of the rich library of trivalent radiometals, in particular ligands to form thermodynamically and kinetically stable *M^{III} complexes are needed. In this context, typical acyclic ligand structures based on the DTPA moiety have been used since decades, also motivated by the use of stable trivalent metals from the lanthanide series applied in MRI imaging as contrast agents. In order to increase the kinetic stability, the structure of the acyclic polyamino-polycarboxylate ligand were translated into cyclic chelators, such as DOTA for many of the radiolanthanides and ^{90}Y. The search for improved ligand structures did never stop, and currently there are e.g. tailored macrocyclic ligands for ^{68}Ga in clinical use based on the triaza scaffold (NOTA, TRAP, etc.). More recent developments contributed new acyclic ligand structures, designed to coordinate ^{68}Ga, such as HBED, DEDPA, THP and oxine-derived acyclic chelating agents. In parallel, a new class of hybrid chelators was developed such as AAZTA (again initially to coordinate Gd^{3+} ion for MRI) and DATA (again tailored towards the requirements of ^{68}Ga coordination).

Excellent articles, such as recent examples, have permanently reviewed these developments.[1] Those reviews discuss the synthesis of the ligands, their bifunctionalization, their coupling chemistry to targeting vectors, and evaluation of complex formation parameters. Critical parameters to consider are the complex formation conditions (pH, temperature, kinetics, concentration of the BFC-Tv compound), as well as stability of the radiolabled conjugate in terms of dissociation of the radiometal from the BFC in vitro and in vivo. A recent development is referred to as "theranostics". In this case, the design of a radiopharmaceutical as illustrated in Figure 1 should be (more or less) identical for both a diagnostic version for PET and SPECT imaging (the radiometal is a photon emitter) and the therapeutic version (the radiometal is a particle emitter). In this case, the chelator should be capable to coordinate both radiometals. In this context, it turns out that DOTA (and its derivatives) currently is the most potent chelator.

[a] *Bracco Imaging spa, Bracco Research Centre, Via Ribes 5, 10010 Colleretto Giacosa (TO), Italy*
[b] *Department of Physical Chemistry, Faculty of Science and Technology, University of Debrecen, Debrecen, Egyetem tér 1, 4032, Hungary*
[c] *Institute of Nuclear Chemistry, Johannes Gutenberg-University of Mainz, Fritz-Strassmann-Weg 2, 55128 Mainz, Germany*
E-mail: frank.roesch@uni-mainz.de
https://www.ak-roesch.radiopharmazie.kernchemie.uni-mainz.de/team/univ-prof-dr-frank-roesch/
ORCID(s) from the author(s) for this article is/are available on the WWW under https://doi.org/10.1002/ejic.201900706.

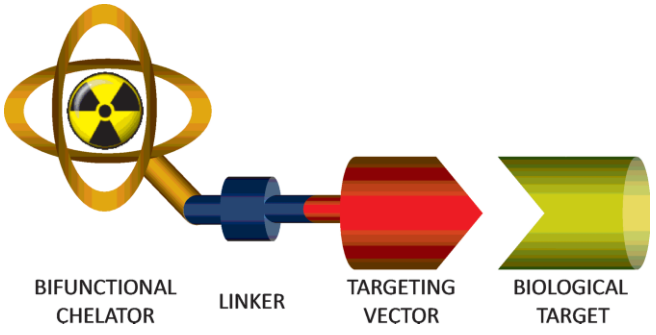

Figure 1. Principal design of a radiopharmaceutical composed of radiometal + BFC + TV to accumulate at a biological target.

However, this review will not go further into the details of the "radiopharmacy and medicine" of radiometal-DOTA-based compounds. In contrast, it is the "non-medical" part of metal-DOTA complexes which is discussed related to the possibility for unique radiochemical separations, i.e. those not possible in conventional chemistry.

Accordingly, this article will first review the physico-chemistry of DOTA and its complexes formed with some trivalent metal ions (M^{III}), which made the DOTA ligand instrumental for contrast agent chemistry in MRI and the dominant chelator in radiopharmaceutical chemistry in nuclear medicine and in theranostics. It will identify one of the main advantages of DOTA in radiopharmaceutical chemistry, the two sites of one (DOTA) coin: efficient complex formation with trivalent radiometals such as ^{68}Ga, ^{44}Sc, ^{90}Y, ^{177}Lu and other radiolanthanides, ^{213}Bi, ^{225}Ac etc. needs elevated temperatures of close to 100 °C, but once the trivalent radiometal is inside the tetraaza core, under room temperature (or human body temperature) it will remain there "forever".

The lesson to learn from those applications of radiometal-DOTA conjugates in live sciences is as follows: complex formation proceeds only at elevated temperatures, but rather slowly at room temperature. Once the radiometal is inside the DOTA cavity, it will remain there at room temperature. Once the radiometal has left the cavity due to nuclear phenomena, it will never return to the complex at room temperature. Consequently, in the second part we will discuss three groups of separations, where radiometal-DOTA complexes are central: the chemical separation of two chemically very similar elements such as two neighbor lanthanides, the chemical separation of two isotopes of the same element, and even the chemical separation of two nuclear levels of the same isotope. Accordingly, DOTA may help to perform radiochemical separations in cases, which for decades appeared to be impossible not only within conventional chemistry, but also within modern radiochemistry.

2. DOTA and its Complexes with Trivalent Metals

2.1 Thermodynamic Stability of the Complexes of Trivalent Metal Ions

Evaluation of a chelator's metal affinity requires knowledge of its acid–base properties (protonation constants) and the thermodynamic stability of its metal complexes. The protonation constant, K_n, is the equilibrium constant for the addition of the R^{th} proton to a ligand, L (for the protonation equilibrium the metal should be omitted in Equation (1). The stability constants of the metal complexes are evaluated through the calculation of formation constants (stepwise constant denoted by K or cumulative formation constants which are marked with β), which

Zsolt Baranyai *was born in Debrecen in 1977. He received his PhD from the University of Debrecen with Prof. Ernő Brücher. After three years postdoctoral fellowship at the University of Torino in the group of Prof. Silvio Aime, he occupied different research positions at the University of Debrecen, where he worked with Prof. Ernő Brücher and Prof. Imre Tóth on the physico-chemical characterization of metal complexes. In 2016, he joined the Bracco Imaging S.p.a. His research activity focuses on the design, and characterization of metal complexes for theranostic applications.*

Gyula Tircsó *was born in Ungvár in 1977. He received his Ph.D. from the University of Debrecen, performing research under the supervision of Prof. Ernő Brücher. In 2004 he joined the group of Prof. A. Dean Sherry at the University of Texas at Dallas (Richardson, Texas, USA) as a postdoctoral research associate. Gyula made a return to academic research at the University of Debrecen where he was appointed a junior lecturer position in 2008, associate professor two years later (in 2010) and assistant professor in 2017. Meanwhile (in 2015) Gyula spent one year at the Center of Molecular Biophysics (CNRS, CBM) in Orleans as a "Le Studium" research fellow under the supervision of Prof. Éva Jakab Tóth. Gyula is an author of 54 journal publications, 3 book chapters and 5 patents. His research activity focuses on the design and characterization of metal complexes (Ln^{III} and transition metal ion based) of biomedical importance.*

Frank Rösch, *born in Chemnitz in 1955, received his PhD from the Technical University of Dresden. After four-year periods of fellowships each at the Joint Institute of Nuclear Research Dubna, the Research Centre Rossendorf, and the Nuclear Research Centre Jülich, he became C4 professor of nuclear and radiopharmaceutical chemistry at the Institute of Nuclear Chemistry, Johannes Gutenberg University Mainz. His research activity focuses on the development of new radionuclides and radiopharmaceuticals for oncology as well as on ^{18}F-tracers for imaging neurotransmission pathways in the human brain.*

are based on the complex equilibrium of metal ions, protons, and ligands (chelators), conventionally written as follows:

$$P{\cdot}M + Q{\cdot}L + R{\cdot}H \rightleftharpoons M_PL_QH_R \quad (1)$$

$$\beta_{PRQ} = \frac{[M_PH_RL_Q]}{[M]^P \cdot [H]^R \cdot [L]^Q}$$

The multidentate ligands generally form mononuclear deprotonated ML complexes at physiological conditions, when the stability constant (K_{ML}) is defined by Equation (2).

$$K = \frac{[ML]}{[M]\cdot[L]} \quad (2)$$

Metal ion affinity of different chelators is commonly compared in terms of logarithm of their stability constants (log K_{ML} = log β_{PQ}) which depends on the ligand basicity thus a more useful parameter is the pM value (pM = –log $[M]_{uncomplexed}$) was introduced for comparative purposes (that express the extent of complexation) by K. N. Raymond and co-workers.[2] pM values for the complexes of trivalent metal ions are generally calculated with the use of following conditions: [L] = 10 μM, [M] = 1 μM, and pH = 7.4. The pM value can be treated as a conditional data, yet it should not be confused with the conditional (effective) stability constant. The conditional stability constant accounts for the competition between the metal and H^+-ion at a given pH and it can be expressed by Equation (3).

$$K_{cond} = [ML]/[M][L]' = [ML]/[M]\{L + HL + H_2L + ...+ H_nL\} = K_{ML}/(1 + \beta_{011}[H] + \beta_{021}[H]^2 + ...+ \beta_{0n1}[H]^n) \quad (3)$$

The determination of the stability constants of metal complexes usually starts with the determination of protonation constants of the ligands. It has to be underlined that the protonation constants are determined by using constant ionic background (some salts like KCl, NaCl, etc.) which has to be selected very carefully as its cation can interact/chelate with the ligand (when the protonation constants are determined) or its counterion may form weak complexes with the metal ion (during the stability constant determination). For instance the Na^+ ion is known to form stable complexes with variety of ligands including DOTA (log $K_{Na(DOTA)}$ = 4.03–4.38)[3] and its derivatives. The K^+ ion containing electrolytes are used less frequently nowadays although it forms weaker complexes with polyaminopolycarboxylate ligands than the Na^+ do. Thus, the protonation constants as well as the stability constants obtained by using Na^+ ion containing medium will always be lower than those obtained with the use of other electrolytes (K^+ or Me_4N^+ salts as it is shown in Table 1 where log β_{021} is the basicity of the macrocyclic nitrogen atoms).[4] This decrease affects the basicity of the ligand, which in turn expect to have an impact on the value of the stability constant. The anion of the salt used to keep the constant ionic strength can also form weak complexes with of the metal ions under question (for instance, Tl^{III} and Bi^{III} are known to form stable halogenido (chlorido, bromido etc.) complexes). By overlooking these competition reactions, the results obtained can be considered as conditional constants only. On the other hand, the majority of the trivalent metal ions form very stable complexes with the DOTA and its derivatives and

Table 1. Protonation constants of the DOTA ligand determined by pH-potentiometry using various ionic strengths (25 °C).

	0.1 M Me_4NCl[7,3b]	0.1 M KCl[8,9]	0.15 M NaCl[10] 1.0 M NaBr[5]
log K_1^H	12.60; 12.09	11.44; 11.14	9.14; 9.01
log K_2^H	9.70; 9.68	9.83; 9.69	9.21; 9.08
log K_3^H	4.50; 4.55	4.38; 4.85	4.48; 4.44
log K_4^H	4.14; 413	4.63; 3.95	4.03; 3.74
log K_5^H	2.32; -	1.92; -	1.99; 1.72
log K_6^H	–; -	1.58; -	–; -
log β_{021}	22.30; 21.77	21.27; 20.83;	18.35; 18.09

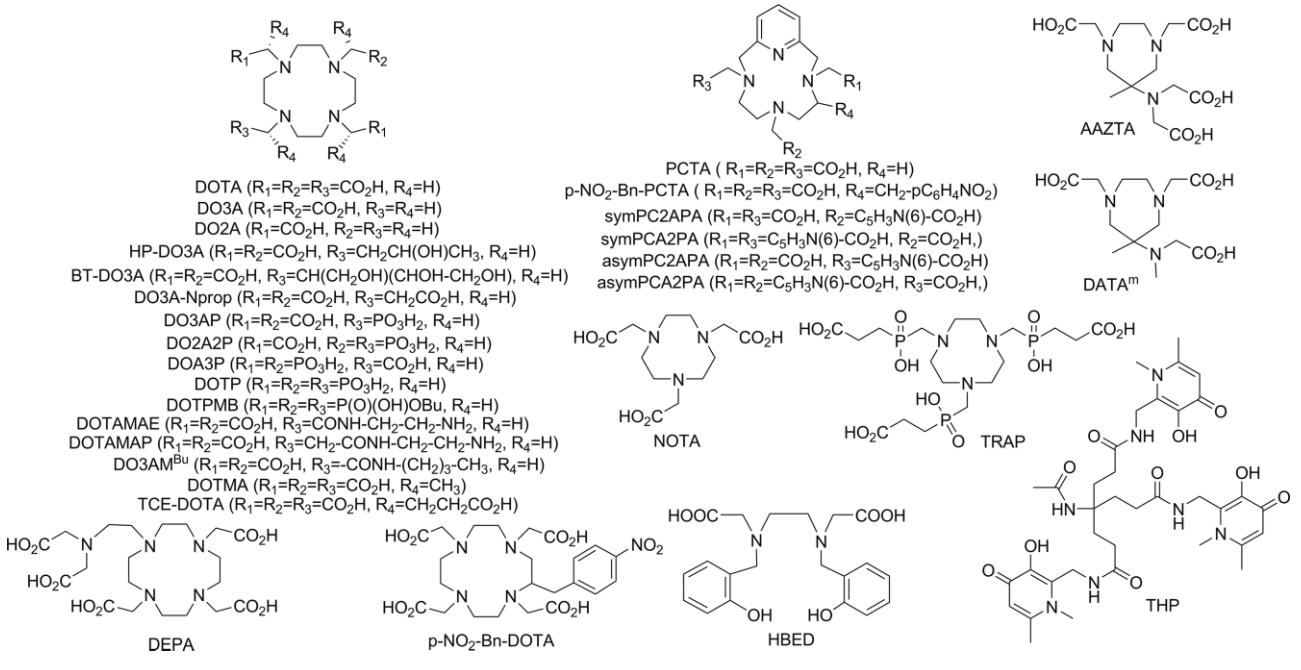

Scheme 1. Structure of the ligands discussed.

there are cases when such competition reactions allow the estimation of large stability constants as they shift the equilibrium in the pH range where it can be followed by more accessible/conventional method(s). In the reaction of Bi^{III} with DOTA for instance, the Bi^{III} ion competes with the H^+ and Na^+ ions (present at high concentration in the sample) for the DOTA ligand while the bromide anion competes with the DOTA ligand (owing to the formation of stable bromido complexes with Bi^{III}). The stability constant of the $[Bi(DOTA)]^-$ was determined to be 30 log units, yet at low pH in the presence of high NaBr concentration (used to set the ionic strength) it can be determined with ease.[5] Using similar approach the stability of the $Tl(DOTA)^-$ complex was also estimated.[6] The chelators mentioned in this paper are shown in Scheme 1.

Linear relationships between experimentally measured log $K_{M(L)}$ values and ligand protonation constants (or basicity) have been reported for nearly 50 years. At first Irving and Rossotti discussed the theoretical basis for such relationships and pointed out reasons why log $K_{M(L)}$ vs. ligand log K_i^H relationships can deviate from linearity even for some simple mono- and bidentate ligands.[11] Later Choppin extended this relationship to include the linear polyamino polycarboxylate systems and demonstrated a single linear correlation between log $K_{M(L)}$ and Σ log K_i^H for monodentate and polydentate ligands that form five-membered chelate rings with Ln^{3+} cations.[12] For the DOTA and DOTA derivatives such a relations works well even for very different classes of ligands (i.e. 1,4,7,10-tetraazacyclododecane derivatives possessing four neutral amide moieties vs. tetraphosphanoate DOTP) when the basicity of the donor atoms present in the macrocycle is plotted vs. log $K_{M(L)}$.[13]

Another important point to bear in mind is that most of the Ln^{III} complexes of macrocyclic ligands tend to form slowly. Some of the Ln^{III} macrocyclic complexes may be prepared only by using extreme conditions such as high temperature, by applying microwave irradiation or application of solvent mixtures etc.[14] Moreover, the formation reactions involving early (Ce^{III}) middle (Eu^{III} or Gd^{III}) and late (Yb^{III}) Ln^{III} ions differ substantially and depend on the structure/type of the ligand (for the DOTA and DOTA-tetramide ligands forming negatively charged and tripositive complexes. Respectively the formation rates along the Ln^{III} series changes even its order. Thus, it is very important to ensure that equilibrium in the samples prepared/used for the stability determinations have attained. For this purpose UV/Vis spectrophotometry (Ce^{III} and Eu^{III}) and NMR (including very convenient T_1 or T_2 relaxometry for Gd^{III}) techniques for the rest of the metal ions is used routinely.[14b,15] Because the complexation kinetics of the DOTA derivatives with Ln^{III} ions are generally slow, the determination of stability constants is fraught with difficulties and the results obtained must be taken with certain precautions. As an illustration, some years ago Desreux and coworkers have plotted the stability constant of Gd(DOTA) complex published in the literature vs. their date of publication.[16] The given plot reviled that most of the studies returned stability constants of about 25 log units for the given complex, but there were hits as low as log $K_{Gd(DOTA)}$ = 22.1 (as determined by kinetic methods)[17] and as high as 27.0 log units (as determined by pH-potentiometry).[18] These data (shown in Table 2) translated into pGd value of 17.5 and 21.0 pointing out the importance of relying on supporting methods when determining such high stability values.[19] Obviously, the most reliable outcome is obtained when different but supportive methods are applied simultaneously (i.e. pH-potentiometric titration data supported by multinuclear NMR (Ga^{III}, In^{III}, Sc^{III}) or T_1/T_2 relaxometry (for the paramagnetic complexes such as Mn^{II} or Gd^{III})) for the stability constant determination. Recently other methods such as high-performance liquid chromatography (HPLC)[20] ion chromatography (IC)[21] and capillary electrophoresis (CE)[22] were also applied for the determination of stability constants of the complexes yet these methods are used less frequently owing to the relatively expensive instrumentation that is not widely available. The stability constants of DOTA complexes formed with some of the relevant (as far as medical imaging concerned) trivalent metal ions are summarized in Table 2.

As it is noted above, data deviating considerably from the ones listed in Table 2 can also be found in the literature however, these disagreements likely arise from the use of inappropriate experimental method(s)/condition(s) or from the measurements performed on not fully equilibrated solutions. It was recognized already in early nineties that the DOTA ligand is robust chelator that form stable and inert complexes with large variety of metal ions. However not all the physico-chemical parameters of these complexes are optimal for applications. For

Table 2. Stability constants of some DOTA complexes formed with some of relevant tripositive metal ions (25 °C). Stability data marked with an asterisk were used to calculate the pM values.[a]

Metal ion	Stability constant	pM	Method
Sc^{III}	27.0;[9] *30.79[23]	23.9	pH-pot. and supported by ^{45}Sc-NMR
Y^{III}	24.3[24] 24.4[24] and *24.9[25]	18.9	pH-pot. capillary isotachophoresis
La^{III}	22.86[26]	18.3	UV/Vis competition with Arsenaso III
Gd^{III}	*24.7[26] 24.67,[3a]25.58[27]	20.1	pH-pot., UV/Vis competition with Arsenaso III, and microcalorimetry
Lu^{III}	25.41[26]	20.8	UV/Vis competition with Arsenaso III
Ga^{III}	21.3,[9] *26.05[28]	15.7	pH-potentiometry supported by Ga-NMR
In^{III}	23.9,[9,29] *24.53[30]	18.8	UV/Vis competition with SHBED and pH-pot.
Tl^{III}	50–60[6]	not calculated	estimation based on UV/Vis
Bi^{III}	30.30[5]	27.0	UV/Vis

[a] Log $K_{M(DOTA)}$; 23.0 (Nd),[26] 23.5 (Eu),[26] 24.2 (Tb),[26] 25.0 (Yb);[26] log K_{ML} values of M(DO3A) complexes: log $K_{Y(DO3A)}$ = 21.1;[31] log $K_{La(DO3A)}$ = 18.63;[8] log $K_{Gd(DO3A)}$ = 21.56;[8] log $K_{Lu(DO3A)}$ = 21.44;[8] log $K_{Bi(DO3A)}$ = 26.85.[32]

instance, some DOTA complexes were found to form very slowly and thus aimed at finding macrocyclic platforms forming complexes more rapidly with therapeutic and diagnostic radioisotopes of were initiated (synthesis of the PCTA, DEPA, sym- and asym-PC2APA and PCA2PA ligands for instance). On the other hand, bioconjugation purposes (i.e. covalent linking of the chelators to taxi molecules such as peptides, antibodies, fragment of antibodies etc.) require bifunctional ligands which are obtained by structural modification of the parent DOTA chelator.

This modification can be done either at the side arm (i.e. DO3A-mono amide derivatives) or at the backbone of the macrocycle (precursors of bifunctional such as p-NO_2-Bn-DOTA, p-NO_2-Bn-PCTA etc. which are studied more often), but either way these structural modifications applied to the parent chelator are expected to affect the physico-chemical parameters of the complexes which needs to be monitored/evaluated.

The stability constants observed across the Ln(III) series for DOTA complexes increase with decreasing of the size of metal ions (Figure 2), The difference between the stability constant of DOTA complexes observed for the largest (La) and smallest (Lu) metal ion is nearly 4 log units. Although is not optimal as there are systems with larger differences in terms of stabilities (i.e. BP18C6 or its rigidified derivatives)[33] yet the given difference might be suitable for the separation of the Ln(III) radioisotopes. Stability constants of the complexes formed with DOTA derivatives such as DO3A-monamides, a structural motif appearing in numerous smart MRI contrast agents as well as in some of the bifunctional ligands (DO3AM^{Bu}: log $K_{Gd(L)}$ = 20.93 in 1.0 M KCl with pGd = 17.8) or DO3A (log $K_{Gd(L)}$ = 21.56 in 0.1 M KCl and 19.06 in 0.15 M NaCl), are generally lower than those of the corresponding DOTA complexes.[8,34] The loss in terms of thermodynamic stability constant is not "earned back" for the complexes, in which the unsubstituted nitrogen atom in DO3A "forced" into a pyridine ring (PCTA). However, Gd^{III} and Y^{III} complexes of PCTA derivatives having one or two picolinate pendant arms possess higher conditional stability than those of the corresponding PCTA complexes in terms of stability they approach the stability of the $[Ln(DOTA)]^-$ complexes.[35] However, the stability constant of the complexes formed with monophosphonate derivatives of DO3A (log $K_{Gd(DO3AP)2-}$ = 27.5) were found to overcome the constants characterizing the $[Ln(DOTA)]^-$ complexes, but again the increase is not substantial if one compare the pGd values ($pGd_{(Gd(DO3AP)2-}$ = 19.0).[36] The addition of a sterically undemanding hydroxypropyl group to DO3A (HP-DO3A) results in a two order of magnitude increase in the stability of the Ln^{III} complexes while addition of the bulky 2,3-dihydroxy-(1-hydroxymethyl)propyl group (to form BT-DO3A) leads to a slight destabilization of its Gd^{III} complex in the comparison with the log K_{GdL} value of [Gd(DO3A)].[37] The 12-membered macrocyclic tetraamine-based DOTA appears to be optimal for Ln^{III} ions. Insertion of one methylene group into the sidearm of the DOTA the DO3AN^{prop} ligand can be obtained. Although the basicity of this ligand is similar to that of DOTA, the stability of the $[Ln(DO3AN^{prop})]^-$ complexes likely (as they are not reported so far) decrease as evidenced by the drop of 6 log units in its Gd^{III} complex stability in comparison to the stability of the $[Gd(DOTA)]^-$ complex.[38]

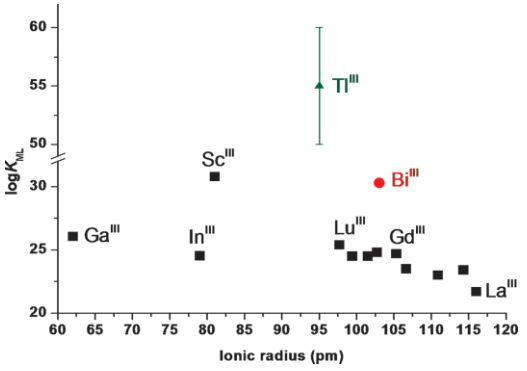

Figure 2. Stability constants of $[M(DOTA)]^-$ complexes as a function of ionic radius.

2.2 Formation Kinetics of DOTA Complexes

In the clinical practice the trivalent M^{III} metal ions are typically chelated by open chain (i.e. DTPA) or macrocyclic (i.e. DOTA) ligands and their derivatives to form highly stable complexes with an aim of avoiding any ligand exchange or transmetalation in the biological milieu (H_5DTPA = diethylene-triamine pentaacetic acid). Although the M^{III} ions forms thermodynamically stable complexes with both type of ligands (see Section 2.1) the formation reactions of metal complexes with the flexible open-chain ligands is generally rapid, whereas the incorporation of metal ions with the rigid macrocyclic ligands is significantly slower process.[39] Rapid complexation is particularly important for radioisotopes with short half-life like ^{68}Ga ($t_{1/2}$ = 67.71 min). In the literature, various conditions (e.g. excess of chelator, different temperatures, pH values etc.) have been proposed for radiolabeling the DOTA-derivatives with ^{68}Ga isotope and other radiometals to improve the labeling yield.[1a,14d,40] However, the conjugation of DOTA derivatives with the temperature and/or pH sensitive targeting vectors such as proteins (e.g. monoclonal antibody) and other taxi molecules require mild complexation conditions, which can strictly limit labeling conditions/procedure. Rapid chelation of the radiometals is one of the key properties being studied and developed in this field.[1a,40f] Although DOTA and its derivatives generally form complexes with M^{III} ions slowly at mild conditions, the safe biomedical applications have been ensured by the high in vivo thermodynamic stability and kinetic inertness of $[M(DOTA)]^-$ complexes. This combination represents the ultimate privilege of the DOTA moiety in radiopharmaceutical chemistry and nuclear medicine.

In order to get insight, the formation kinetics and mechanisms of DOTA-like complexes with trivalent metal ions have been overviewed by taking into account the effect of the ligand structure, donor atoms and metal ions for the rate of the reactions. The M^{III} complexes of DOTA and its derivatives are often form slowly because the metal ion must enter into the preorganized coordination cage formed by the nitrogen atoms of the macrocycle and by the oxygen atoms of the pendants.[41] The kinetic studies showed that the formation of DOTA complexes with Ln^{III} ions occurs through the diprotonated $^{\#}[Ln(H_2DOTA)]^+$ intermediate in which the metal ion is coordinated only by the deprotonated carboxylate oxygen atoms of

the pendant arms.[42] The formation and the structure of the diprotonated $^{\#}[Ln(H_2DOTA)]^+$ intermediate has been examined by spectrophotometry,[15] ^{1}H-NMR,[17] luminescence spectroscopy,[43] and EXAFS.[27] Moreover, due to the slow rearrangement at pH < 4, the composition and the stability constants of the diprotonated $^{\#}[Ln(H_2DOTA)]^+$ intermediates could be determined by pH-potentiometric titration.[8,15,43b] Similar diprotonated $^{\#}[Ln(H_2L)]^+$ intermediates formed by several other DOTA derivatives have been identified and characterized in terms of structure, composition and stability constants.[8,44] Several divalent metal ions form complexes with DOTA ligand through protonated intermediates.[45] Based on the proposed structure of the $^{\#}[Ln(H_2DOTA)]^+$ intermediate, Ln^{III} ion is situated outside the coordination cage by the coordination of four carboxylates, whereas the two protons are attached to two *trans*-nitrogen atoms of the macrocyclic ring.[15,43b] Luminescence decay studies of the $^{\#}[Eu(H_2DOTA)]^+$ intermediate reveal the presence of four or five water molecules in the inner-sphere of the Eu^{III} ion.[43] The deprotonation of the diprotonated $^{\#}[Ln(H_2DOTA)]^+$ intermediate by the formation of the monoprotonated $^{\#}[Ln(HDOTA)]$ intermediate might also take place at higher pH values (pH > 7) in equilibrium reaction. According to the well-established mechanism, the rate-determining step for the formation of Ln^{III} complexes with DOTA is the loss of the last proton from the $^{\#}[Ln(HDOTA)]$ intermediate followed by the rearrangement of the fully de-protonated intermediate to the final "in-cage" complex (Figure 3).[3a,17,46] Similar interpretation has been proposed for the formation of M^{III} complexes of other DOTA-like ligands.[14b,27,43a,44b,44c] In the deprotonation of the monoprotonated $^{\#}[Ln(HDOTA)]$ intermediate, the proton from the ring nitrogen transfers to the bulk water or OH^- ion by the possible assistance of a carboxylate side arm in the general base catalyzed process.

Because of the $^{\#}[Ln(H_2DOTA)]^+ = {}^{\#}[Ln(HDOTA)] + H^+$ equilibrium of the intermediates, the formation of the $[Ln(DOTA)]^-$ complexes through the monoprotonated intermediate is directly proportional to the OH^- ion (or $1/[H^+]$) concentration. The detailed kinetic studies reveal that the rate-controlling step is the deprotonation of the monoprotonated $^{\#}[Ln(HDOTA)]$ intermediates by H_2O as a weak Bronsted base (k_{H2O}) and OH^- assisted (k_{OH}) pathways in the formation of Ln^{III} complexes with DOTA and its derivatives.[7,14b] Similar mechanism has been proposed for the formation of other trivalent metal complexes with DOTA and its derivative ligands.[14b] k_{OH} rate constant for the formation of several Ln^{III} complexes with DOTA derivatives are shown in Table 3.

Table 3. Formation rate constants k_{OH} (M^{-1} s^{-1}) of the DOTA derivative complexes.[a]

Ligand	Ce^{III}	Eu^{III}	Gd^{III}	Yb^{III}
DOTA [15]	3.5×10^6	1.1×10^7 7.2×10^6 [43b] 2.0×10^7 [47]	5.9×10^6 [46]	4.1×10^7 9.3×10^7 [46]
DO3A [46]	–	–	2.1×10^7	
DO2A [44b]	2.8×10^5	–	–	2.5×10^5
HP-DO3A [46]	–	–	1.2×10^7	–
BT-DO3A [44b]	2.1×10^6	4.8×10^6	–	1.6×10^7
DO3A-Nprop[38]	1.7×10^7	–	2.9×10^7	3.9×10^7
PCTA [48]	9.7×10^7	1.7×10^8	–	1.1×10^9
NO_2-Bz-PCTA[49]	1.0×10^7	1.4×10^8	–	5.6×10^8
DO3AP [44c]	9.6×10^6	2.7×10^6, [43a]	9.0×10^4	–
DO2A2P [50]	1.7×10^5	–	6.6×10^4	–
DOA3P [51]	–	–	2.2×10^4	–
DOTP [52]	–	–	7.2×10^3	–
DOTPMB [52]	–	–	1.3×10^3	–
DOTAMAE [53]	9.7×10^5	1.2×10^7	–	–
DOTAMAP [53]	2.7×10^6	2.8×10^7	–	–

[a] Some other k_{OH} values: 1.3×10^{11} M^{-1} s^{-1} ($[Ga(DOTA)]^-$), 4.8×10^9 M^{-1} s^{-1} ($[Y(DOTA)]^-$) and 1.1×10^9 M^{-1} s^{-1} ($[Lu(DOTA)]^-$).[14b]

The k_{OH} values presented in Table 3 show some correlations for the formation rates and the nature of the Ln^{III} ion as well as the structure of ligand. Removal of the carboxylate groups (DO3A, DO2A) or the substitution of a non-charged alcohol/polyalcohol (HP-DO3A, BT-DO3A) or amide group (DOTAMAE, DOTAMAP) for the carboxylate groups results in a slight decrease of the formation rates of Ln^{III} complexes. On the other hand, the presence of the propionate instead of one acetate side-arm of DOTA results in the somewhat faster formation of $[Ln(DO3A\text{-}Nprop)]^-$ complexes than those of the corresponding $[Ln(DOTA)]^-$ analogues.[38] The k_{OH} values characterize the formation of Ln^{III} complexes with DOTA derivatives possessed by carboxylate pendants increase with the decrease of the size of Ln^{III} ions. Although the formation mechanism of $[Ga(DOTA)]^-$ and $[Ln(DOTA)]^-$ complexes seems to be similar, the OH^- assisted formation of $[Ga(DOTA)]^-$ is about 100 times faster than that of $[Ln(DOTA)]^-$ complex.[14b] On the other hand, the formation rate (k_{OH}) of $[Ln(DO3AP)]^{2-}$ and $[Ln(DO2A2P)]^{3-}$ complexes decreases with the decrease of the size of Ln^{III} ions. By taking into account the different formation rates, the DOTA and its derivative ligands might discriminate M^{III} ions based on their size in the radiochemical sequestration.

Interestingly, the formation of $[Ln(DOTA)]^-$ complexes is about one order of magnitude slower than that of the corresponding [Ln(PCTA)] complexes, which can be explained by the

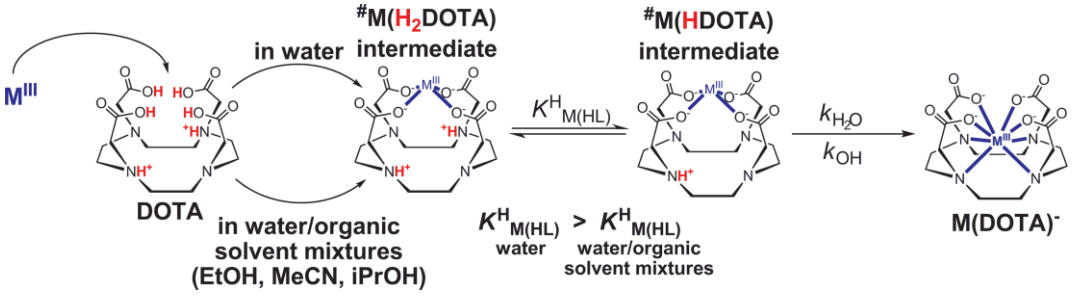

Figure 3. Formation of $[M(DOTA)]^-$ complexes. Adapted with permission from ref.[14b] Copyright (2018) American Chemical Society.

more pre-organized structure of the PCTA ligand due to the presence of the pyridine moiety.[48] Moreover, the attachment of the NO_2-Bn- moiety to the PCTA backbone for the conjugation purposes with biological active molecules does not seem to alter the favorable formation kinetic properties of [Ln(PCTA)] complexes.[48,49] By taking into account the faster formation and the sufficiently high kinetic inertness, the [Ln(PCTA)] complexes are promising alternatives of $[Ln(DOTA)]^-$ complexes for in vivo applications.

To improve the preorganization of the ligand, several DOTA derivatives possessing α-substituted pendants (e.g. DOTMA, TCE-DOTA) have been developed.[54] However, the k_{OH} value characterize the formation of $[Eu(DOTMA)]^-$ complex is about 3 orders of magnitude smaller than that determined for $[Eu(DOTA)]^-$, which indicates that the rigidity of the pendants slows down the formation of the Ln^{III} chelates.[54] Similar approach has been adapted when designing chiral DOTA chelates with the symmetrically arranged substituents (Me, Et, Bn, *i*Bu) attached to the tetraaza core with an aim of locking the conformation of the chelator.[1f] The comparison of the labeling efficiency revealed that the incorporation of $^{177}Lu^{III}$ isotope with the ethyl C-substituted ligand is faster than it was observed for the parent DOTA, which confirms the key role of the conformation of the macrocycle ring in the formation of the complex.

The k_{OH} values of the Ln^{III} complexes formed with DOTA derivatives possessing mixed carboxylate-phosphonate pendant arms decrease with the gradual replacement of the carboxylate arms by the phosphonate groups, which can be explained by the stabilization of the $^{\#}Ln(H_2L)$ intermediate due to the higher negative charge on the pendant arm. The kinetic studies of PCTA-like complexes possessing with mixed carboxylate and picolinate side chains reveal that the formation rates of the Ln^{III} complexes with the non-symmetric monoacetate-dipicolinate and monopicolinate-diacetate derivatives is significantly faster than the formation rates of the complexes of symmetrical regioisomers.[35] These findings were explained in terms of labile capping bond effect in lanthanide complexes.

It was recently shown that the presence of ethanol in mixtures utilized to purify $^{68}Ge/^{68}Ga$-generator eluates substantially increases the radiolabeling efficacies for [^{68}Ga]Ga-DOTA-TOC derivatives in comparison with pure aqueous solutions.[55] Moreover, the formation of [^{68}Ga]Ga(DOTA), [^{44}Sc]Sc(DOTA) and [^{177}Lu]Ga(DOTA) complexes in water/organic solvent (EtOH, MeCN or *i*PrOH) mixtures is significantly faster than in pure aqueous solution.[14b] The detailed kinetic studies on the formation of $[M(DOTA)]^-$ (M = Ga^{III}, Ce^{III}, Eu^{III}, Y^{III} and Lu^{III}) complexes reveals that the mechanism of complex formation between M^{III} ions and DOTA ligand is very similar in water and water/ethanol mixtures (up to 70 vol.-% EtOH).[14b] In the reaction of M^{III} ions with DOTA ligand, the formation of diprotonated $^{\#}[M(H_2DOTA)]^+$ intermediate can also be detected by spectrophotometry and ^{1}H-NMR spectroscopy in water/ethanol mixtures. The formation of the $[M(DOTA)]^-$ complexes in water/ethanol mixtures occurs through the rate-controlling deprotonation and rearrangement of the monoprotonated $^{\#}[M(HDOTA)]$ intermediates formed in equilibrium with the diprotonated $^{\#}[M(H_2DOTA)]^+$ intermediates (Figure 3). The EtOH indirectly accelerates the formation of $[M(DOTA)]^-$ complexes by decreasing the protonation constant ($K^H_{M(HL)}$, Figure 3) of the kinetically active monoprotonated $^{\#}[M(HDOTA)]$ intermediates that results in the faster formation of the final complex. The presumed decrease of the $K^H_{M(HL)}$ values with increasing EtOH concentration can be interpreted by the decrease of the basicity of the ring N donor atoms in the $^{\#}[M(H_2DOTA)]^+$ intermediates.[14b] This assumption is based on the observation that the basicity of the macrocyclic N donor atoms of the free DOTA ligand characterized by log K_1^H and log K_2^H protonation constants decrease with increasing EtOH concentration.[14b]

2.3 Dissociation Kinetics of DOTA Complexes

The kinetic inertness of metal complexes represents a key requirement for their in vivo applications, which means they practically should not release metal ion and ligand once administered into the body. To ensure the full elimination from the living system, stable and kinetically inert Gd^{III} complexes are commonly used as contrast agents in Magnetic Resonance Imaging, whereas luminescent complexes of Eu^{III} and Tb^{III} characterized by high thermodynamic stability and kinetic inertness have frequently utilized in fluoroimmunoassays and as luminescent probes for Optical Imaging.[56] The radiometal complexes formed with bifunctional chelates covalently coupled to proteins or monoclonal antibodies, used for radiodiagnosis or radiotherapy, must be also highly inert. Depending on the biological targeting vector, the carriage of the radiopharmaceuticals to the target site could be very slow and the kinetic inertness of the radiometal complexes should guarantee the chelation of the radioisotope in order to avoid the loss of therapeutic efficiency of the treatment and the free radioisotope generated damage of the healthy organs. Based on the generally accepted mechanism of the in vivo dechelation, the loss of the metal ions and ligands from metal complexes might take place by the transmetallation reactions with endogenous metal ions (Zn^{II}, Cu^{II}, Ca^{II}, Fe^{III}) and by ligand exchange reactions, when an endogenous ligand (transferrin, PO_4^{3-}, CO_3^{2-}) displaces the chelating agent. The kinetics of metal and ligand exchange reactions of amino-polycarboxylate complexes formed with transition metal-, Ln^{III}-, Y^{III}- and Sc^{III}-ions have been investigated in the last 40–50 years.[39] In the $[M(DOTA)]^-$ complexes, the M^{III} ion is located in the coordination cage formed by the four macrocyclic nitrogen and four carboxylate oxygen atoms, which can hinder the interactions with other multidentate ligands due to the completed coordination sphere of M^{III} ion. Moreover, the carboxylate groups in $[M(DOTA)]^-$ complexes are not flexible enough to be transferred to an exchanging metal ion. In agreement with these assumptions, the detailed kinetic studies of the transmetallation reactions between $[Gd(DOTA)]^-$ and [Gd(HP-DO3A)] complexes and Cu^{II} in the presence and absence of citrate and phosphate ligands reveal that the concentration of Cu^{II} and endogenous ligands does not affect the dissociation rates of complexes.[57] However, the proton can successfully compete with the M^{III}-ion for the interaction with donor atoms in DOTA ligand that results in the formation of protonated $M(H_xL)$ complexes (x = 1 for Ln^{III}, Y^{III} and Sc^{III}, x = 2 for Ga^{III}),

which is the first step in the dissociation $[M(DOTA)]^-$ complexes. ^{1}H-NMR studies indicate the protonation of $[Lu(DOTA)]^-$ complexes on the non-coordinated oxygen of the carboxylate group bound to Lu^{III} ion.[58] The X-ray structure of $[Ga(H_2DOTA)]^+$ complex shows that Ga^{III} ion is coordinated by four macrocyclic nitrogen and two carboxylate oxygen atoms, while two non-coordinated carboxylate oxygen atoms remain protonated because the Ga^{III} ion has a coordination number of 6.[28] The protonation constant of the $[M(DOTA)]^-$ complexes characterized by $K_{M(HxL)}$ value is relativley low ($K_{M(HxL)}$ = 10–400 M^{-1}) due to the strong interaction between the M^{III} ions and the carboxylate oxygen atoms. The log $K_{M(HxL)}$ values of the $[M(DOTA)]^-$ complexes are comparable with the log K_5^H and log K_6^H values of free DOTA ligand (Table 1), which also suggests that the protonation of $[M(DOTA)]^-$ complexes takes place on the carboxylate group/s. In the protonated $M(H_xL)$ complex the carboxylate group might become free, but the resulting protonated complex is not reactive, since the protonation/deprotonation step of the carboxylate group is fast and the COO^- group can be bound again. Dissociation is more probable by the transfer of proton from the carboxylate group to one of the macrocyclic nitrogen atoms, resulting in the formation of labile protonated intermediate in which the proton may displace the M^{III} ion followed by the protonation of the second diagonally positioned nitrogen atom in the macrocycle. As was shown in Figure 3 (Section 2.2), the diprotonated $^{\#}[M(H_2DOTA)]^+$ intermediate formed by the interaction between M^{III} and H_2DOTA^{2-} in equilibrium has an important role for the formation of $[M(DOTA)]^-$ complexes. However, the dissociation of the diprotonated $^{\#}[M(H_2DOTA)]^+$ intermediate is also probable by the release of the free M^{III} ion and H_2DOTA^{2-} ligand.

The kinetic internets of $[M(DOTA)]^-$ complexes are characterized either by the rates of their dissociation measured in $[H^+]$ range of 0.05–1.0 M or by the rates of transmetallation reaction, occurring in solutions with Zn^{II} and Cu^{II} or Eu^{III} by spectrophotometry, fluorescence spectroscopy, multinuclear NMR spectroscopy and chromatography methods.[15,17,59] The first-order rate constants (k_d) characterizing the dissociation of the $[M(DOTA)]^-$ complexes are generally independent from the concentration of the exchanging metal ions. However, the k_d rate constants are directly proportional to $[H^+]$ and k_d can be expressed by Equation (4):

$$k_d = k_0 + k_1[H^+] \quad (4)$$

where k_0 and k_1 are the rate constants characterizing the spontaneous and proton-assisted dissociation of $[M(DOTA)]^-$ complexes, respectively. In more acidic solution ($[H^+]$ > 0.3 M), the k_d shows an saturation or exponential tendency as a function of $[H^+]$, which can be explained by the accumulation of the monoporotonated $^{\#}[M(HDOTA)]$ intermediate and by the protonation of two carboxylate groups and the formation of diprotonated $^{\#}[M(H_2DOTA)]^+$ intermediate characterized by significantly lower inertness.[15,60] At physiological condition, the dissociation of $[Ln(DOTA)]^-$ complexes mainly occur through the formation and the dissociation of the monoprotonated $^{\#}[Ln(HDOTA)]$ intermediate characterized by very low k_1 rate constant values. The k_1 rate constant of several DOTA-like complexes formed with Ln^{III} ions are presented in Table 4.

Table 4. Rate constants k_1 (M^{-1} s^{-1}) characterizing the proton assisted dissociation of the DOTA derivative complexes (25 °C).[a]

Ligand	Ce^{III}	Eu^{III}	Gd^{III}
DOTA	8×10^{-4} [42]	1.4×10^{-5} [43a]	8.4×10^{-6} [17]
	3.4×10^{-4} [61]		1.8×10^{-6} [61]
			2.0×10^{-5} (37 °C) [15]
			3.6×10^{-5} (37 °C)[62]
DO3A[60]	1.1×10^{-1}	–	2.6×10^{-3}
			1.2×10^{-2} [59a]
			2.3×10^{-2} [8]
HP-DO3A	2.0×10^{-3} [60]	–	6.4×10^{-4} [60]
			2.6×10^{-4} [37]
			2.9×10^{-4} [57]
BT-DO3A [37]	–	–	2.8×10^{-5}
DO3A-Nprop [38]	7.3×10^{-3}	–	–
PCTA [48]	9.6×10^{-4}	5.1×10^{-4}	2.8×10^{-4} (Yb^{III})
p-NO_2-Bz-PCTA[49]	4.8×10^{-5}		1.7×10^{-4}
DO3AP [44c]	1.2×10^{-3}	9.8×10^{-5} [43a]	2.8×10^{-3}
DO2A2P [50]	3.5×10^{-4} [63]	5.2×10^{-4} [63]	1.9×10^{-4}
DOA3P [51]	2.4×10^{-4} [64]	2.35×10^{-4} [64]	2.7×10^{-4}
DOTP [52]	4.6×10^{-2} [43a]	1.3×10^{-3} [43a]	5.4×10^{-4}
DOTPMB [52]	–	–	2.1×10^{-4}
DOTAMAE [53]	–	–	2.6×10^{-6}
DOTAMAP [53]	–	–	2.1×10^{-3}

[a] Some other k_1 values: 6.0×10^{-7} M^{-1} s^{-1} ($[Ga(DOTA)]^{2-}$),[28] 1.0×10^{-6} M^{-1} s^{-1} ($[Ga(DO3AM^{Bu})]^-$)[28] and 6.0×10^{-6} M^{-1} s^{-1} ($[Sc(DOTA)]^-$).[23]

The comparison of the k_1 data summarized in Table 4 indicates that the rate of the acid catalyzed dissociation of Ln^{III} complexes formed with DOTA derivatives are strongly influenced by the size of the Ln^{III} ion as well as the structure of ligands. The k_1 values of Ce^{III}, Eu^{III} and Gd^{III} complexes of DOTA decrease with the decrease of the size of Ln^{III} ion, which might be interpreted by the better size match between the Gd^{III} ion and the coordination cage offered by the DOTA ligand.

The dissociation rate of Ln^{III} complexes with octadentate DOTA derivatives are slower than those of the heptadentate DO3A and PCTA complexes due to the easy protonation on the secondary and pyridine nitrogen of DO3A and PCTA ligand than on the tertiary nitrogen of DOTA.[48,59a,60] On the other hand, the kinetic studies on PCTA-like complexes with mixed carboxylate-picolinate side chains reveal that the acid-catalyzed dissociation of the Gd^{III} complexes with the non-symmetric and symmetric monoacetate -dipicolinate pendants are significantly slower than the complexes formed with the non-symmetric and symmetric monopicolinate-diacetate regioisomers.[35] The replacement of the carboxylate group by the weaker coordinating –OH group results in the lower kinetic inertness of the [Gd(BT-DO3A)] and [Gd(HP-DO3A)] complexes. The somewhat slower proton-assisted dissociation of [Gd(BT-DO3A)] can be explained by its more polarized –OH group, characterized by lower dissociation constant than that of [Gd(HP-DO3A)] ([Gd(BT-DO3A)]: log K_d = 9.48; [Gd(HP-DO3A)]: log K_d = 11.36).[37]

Gradual substitution of phosphonate groups for the carboxylate groups of DOTA leads to the formation of Ln^{III} complexes characterized by lower kinetic inertness. The higher k_1 values are more likely caused by the higher basicity of the non-coordinated oxygen (protonation of the non-coordinated phosphonate oxygen in the complex occurs at pH = 5–7) that results in the intramolecular proton transfer to the coordinated oxygen

of the phosphonate group/s which leads to in the dissociation of Ln^{III} complex. The proton-assisted dissociation of the Ln^{III} complexes possessed by two, three or four phosphonate groups is more probable because of the formation of several protonated intermediates that promotes the proton transfer to the ring nitrogen atoms and thus the displacement of Ln^{III} ion from the coordination cage effectively.

Interestingly, the replacement of the negatively charged acetate pendant by the neutral acetamide functionality in DOTA does not influence the rate of the proton catalyzed dissociation of [Gd(DOTAMAE)], whereas the introduction of a propionamide or propionate side-arm by the substitution of the acetate group results in the significant drop of the kinetic inertness of the corresponding Ln^{III} complexes. This is presumably because the weaker amide and carboxylate oxygen – Ln^{III} interactions in the six-membered chelate ring upon the coordination of Ln^{III}-ion.[38,53]

The kinetic inertness of the Ln^{III} complexes formed with DOTA derivatives with enhanced rigidity reveals that the rate of the acid catalyzed dissociation significantly decreases with the increased ligand preorganization (i.e. coordination cage) by the presence of α-substituted pendants (e.g. DOTMA, TCE-DOTA)[54] and alkyl substituents attached to the tetraaza core (i.e. chiral DOTA chelates).[1f]

There is an intense scrutiny for the effect of the linker and targeting vector on the kinetic inertness of the resulting complexes in the development of bifunctional ligands. However, only few systematic studies have been performed for the kinetic characterization on the dissociation reactions of Ln^{III} complexes formed with DOTA and PCTA bifunctional analogues. Based on the available kinetic data the k_1 values of the complexes of DOTA and p-NO_2-Bn-DOTA, PCTA and p-NO_2-Bn-PCTA are very similar.[49,65] Moreover, the bifunctional analogues are characterized by similar kinetic inertness to those of the parent phosphonate and phosphinate derivatives of DOTA complexes.[36,66] The rate of acid-assisted dissociation of Ln^{III} complexes formed with DOTA DO3A, PCTA and several phosphonate and phosphinate derivatives of DOTA are very similar to those in the case of Y^{III}, Sc^{III}, Bi^{III} and Ga^{III} complexes, which confirms their satisfactory inertness for the application in nuclear medicine.[32,36,48,59a,67]

It is worth to note that Ga^{III} and Bi^{III} ions show a strong affinity to hydroxide ions and all known Ga^{III} and Bi^{III} complexes decompose in alkaline media forming the $[Ga(OH)_4]^-$ and $[Bi(OH)_4]^-$ anion.[68] The detailed kinetic investigations of $[Ga(DOTA)]^-$, $[Ga(DO3AM^{Bu})]$ and [Bi(DO3A)] reveal that the dissociation of Ga^{III} and Bi^{III} complexes may take place by the OH^- assisted pathway via the formation of mono-hydroxo [Ga(L)OH] and [Bi(L)OH)] complexes. The formation and dissociation of mono-hydroxo [Ga(L)OH] and [Bi(L)OH)] complexes is characterized by the k_{OH} rate constant. The comparison of the k_{OH} and k_1 rate constants of Ga^{III} and Bi^{III} complexes indicates that the OH^- assisted dissociation is significantly faster than that of the proton-assisted decomplexation, which confirms the important role of the hydroxide-assisted dissociation at pH ≥ 7.[28,32] By taking into account the different dissociation rates and mechanisms, the kinetic inertness of $[M(DOTA)]^-$ complexes might allow the radiochemical separation of $*M^{III}$ isotopes when the conditions selected accurately .

3. DOTA in MRI

The interest in the unique complexation properties of macrocyclic ligands has gained the synthesis and characterization of several new cyclic polyoxa and polyaza ligands. In 1976 Stetter and Frank reported that the DOTA ligand forms the most stable Ca^{II} complex among the macrocyclic ligands.[69] By taking into account the similarity between the Ca^{II} and trivalent rare earth metal ions in terms of size and high affinity to carboxylate oxygen donor atoms, it was proposed that the DOTA would be an excellent chelating agent of the trivalent rare earth metal ions. Based on this assumption, the systematic studies of the Ln^{III} complexes formed with DOTA had been performed in early 80s. The first Ln^{III} complex of DOTA was published by Bryden et al. in 1981,[70] which is followed by the detailed equilibrium, kinetic and structural investigations of $[Ln(DOTA)]^-$ complexes.[17,26,41,42,71] It was found that DOTA is one of the most powerful chelating agent of trivalent rare earth metal ions, which opened up the application of DOTA as chelating agents of the paramagnetic lanthanide metal ion, gadolinium(III) for the development of contrast agent in Magnetic Resonance Imaging (MRI).

The complexes of Gd^{III} formed with the open-chain DTPA, the macrocyclic DOTA and their derivatives are widely used as MRI contrast agents from the end of the 80s. In MRI investigations $[Gd(DOTA)(H_2O)]^-$ was first used by Magerstadt and Caille in 1986.[72] $[Gd(DOTA)(H_2O)]^-$ (DOTAREM® is the trade name of the pharmaceutical with 0.5 mol/dm³ NMG[Gd(DOTA)(H_2O)]) has been a first generation extracellular MRI contrast agent. Based on the promising results for the in vivo use of $[Gd(DOTA)(H_2O)]^-$, numerous DOTA based MRI contrast have been developed by taking into account several important issues: high solubility, high efficiency, low toxicity, low osmotic pressure, high thermodynamic and kinetic stability of the Gd^{III} complexes and the presence of at least one water molecule coordinated to the Gd^{III} ion to transfer the paramagnetic effect to the bulk via exchange processes[73] As nonionic contrast agents, Gd^{III} complexes formed with 1,4,7,10-tetraazacyclododecane-1,4,7-triaacetic acid (DO3A) have been proposed in order to reduce the osmotic pressure.[60] The first macrocyclic non-ionic contrast agent introduced into clinical use was ProHance® (0.5 mol/dm³ [Gd(HP-DO3A)(H_2O)] formulated with 0.1 % Na[Ca(HP-DO3A)]) in which the Gd^{III} has been complexed by HP-DO3A ligand (HP-DO3A = 10-(2-hydroxypropyl)-1,4,7,10-tetraazacyclododecane-1,4,7-triacetic acid.[31,46,60,74] The next non-ionic extracellular contrast agent proposed for the clinical application in MRI was GADOVIST® (1.0 mol/dm³ [Gd(BT-DO3A)(H_2O)] formulated with 0.1 % Na[Ca(BT-DO3A)]) in which the Gd^{III} ion is chelated by BT-DO3A ligand (BT-DO3A = 10-[2,3-dihydroxy-(1-hydroxymethyl)propyl]-1,4,7,10-tetraaza-cyclododecanc-1,4,7-triacetic acid).[75] As it is well known that MRI is a relatively insensitive modality, the required dose of the contrast agents is rather high (0.1 mmol/kg body weight) due to the low efficiency of the clinically used Gd^{III} complexes. The efficiency

is characterized by the longitudinal proton relaxivity (r_1, the increase in the water proton relaxation rate per mM concentration of Gd^{III}) which, for the clinically approved Gd^{III} complexes, lies in the range 4–5 mM^{-1} s^{-1}, at 20 MHz (0.47 T) and 298 K. In order to increase the efficacy, it is necessary to develop the Gd^{III} complexes characterized by high relaxivity. Over the last 20–30 years, Gd^{III}-chelates have been under intense scrutiny to design new systems whose structural, dynamic and relaxation properties correspond to the characteristics of high relaxivity agents through the optimization of the molecular parameters that control the magnetic coupling between the paramagnetic ion and water molecules (e.g. hydration number, rotational correlation time of the Gd^{III} – proton vector and residence time of the water molecule in the inner-sphere of Gd^{III} ion).[76]

The development and chemistry of Gd^{III} based MRI contrast agents are summarized in several reviews,[73,77] book chapters[76,78] and books.[13,79] Attention has been mainly focused on the following activities: *i)* Gd^{III} complexes containing two coordinated water molecules (e.g. $[Gd(DO3A)(H_2O)_2]$, $[Gd(PCTA)(H_2O)_2)]$ and their derivatives;[80] *ii)* control of the molecular tumbling (e.g. $[Gd(DOTA)(H_2O)]$-like structures bearing bulk substituents);[81] *iii)* improved contribution from water molecules in the 2nd coordination sphere (e.g. $[Gd(DOTP)]^{5-}$);[82] *iv)* targeting human serum albumin,[53,83] fibrin,[84] collagen type I,[85] amyloid-β peptides[86] $\alpha_v\beta_3$ integrin[87] and high-affinity folate receptors;[88] *v)* improving the local concentration of paramagnetic metal centers, linking the single chelates in multimeric systems[89] or collecting them in well-defined nanoparticles.[90]

On the other hand, the modification of the pendant arms on DOTA allows the design of the MRI contrast agents for molecular imaging applications in which imaging probes are required to report specific physical or (bio)chemical parameters (e.g. pH,[8,91] pO_2[92] the concentration of glucose[93] metal ions,[94] redox potential[95] and enzymes[96]) gained to an extensive research of responsive MRI probes.[97] By taking into account the development in the last 50 years, numerous Gd^{III} complexes formed with DO3A- and DOTA-like ligands have been designed and synthesized for their potential application as MRI contrast agents. The fine-tuning of the various determinants has allowed the discovery of Gd^{III} complexes characterized by higher efficiency than that shown by the clinically used Gd^{III}-base contrast agent without the alteration of the high thermodynamic stability and kinetic inertness. Moreover, Gd^{III}-based "responsive" MRI probes as powerful tools available for Molecular Imaging applications can be the reporter the given physico-chemical parameter of the micro-environment where they are distributed.

4. DOTA in the Life Sciences: A "Theranostic" Chelator

DOTA was the first macrocyclic chelator introduced to design radiometal-based diagnostics and therapeutics. Today, several bifunctional versions of DOTA are established in addition to DOTA-conjugated radiopharmaceuticals based on DO3A coupling to targeting vectors forming amide bonds of one of the four carboxyl groups with NH_2-functionalities of the targeting vector, such as e.g. DOTAGA versions using an additional carboxy functionality added to the DOTA core, dimeric variants of DOTA allowing for asymmetric substitution of two identical or two different targeting vectors (see e.g.[98]) to one DOTA core. Those *M-DOTA-conjugated radiopharmaceuticals dominate the spectrum of compounds used in nuclear medicine diagnosis and therapy, although for individual radionuclides such as $^{68}Ga^{III}$ or $^{64}Cu^{II}$ new chelators (macrocyclic, semi-macrocyclic and non-macrocyclic) and their bifunctional derivatives have been developed, such as NOTA and NODAGA and TRAP (macrocyclic),[99] THP (non-macrocyclic),[100] AAZTA and $DATA^m$ (semi-macrocyclic or "hybrid")[101] and others.

One of the good reasons to consider DOTA as in particular relevant lies in the new era of THERANOSTICS. According to the philosophy of THERANOSTICS applied to radiopharmaceutical chemistry and nuclear medicine, an almost identical chemical structure of the diagnostic version and the therapeutic counterpart of a lead structure targeting the same disease is its ideal. For the same targeting vector (such as e.g. a tumor affine peptide) and the same chelator, this particular chelator shall stably coordinate both a positron emitter for pre-therapeutic PET diagnosis, and a chemically (almost) identical particle emitter for treatment. It is obvious that, among all the chelates investigated, indeed DOTA offers the best options for the latter aspect. There is a number of radiometals providing different emission characteristics, and – although being chemically different - nevertheless fit into the DOTA coordination chemistry. Figure 4 illustrates the many radionuclides (and there may be even some more candidates to mention) that all are known to work within various DOTA conjugated radiopharmaceuticals.

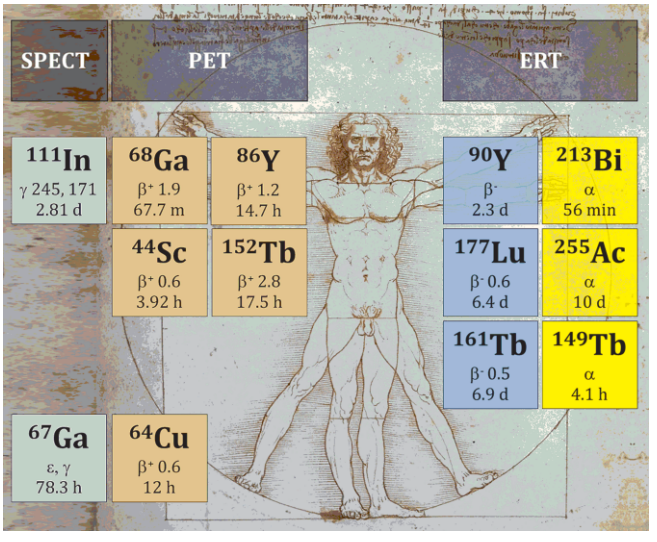

Figure 4. Radionuclides known to work within various DOTA conjugated radiopharmaceuticals allowing for SPECT and PET molecular imaging and for endoradiotherapy.

Accordingly, several diseases are covered by the theranostic strategy using DOTA-conjugated targeting vectors. The first example to mention is the diagnosis and therapy of neuroendocrine tumors using DOTA-conjugated octreotide derivatives such as DOTA-TOC and DOTA-TATE. Historically, ^{111}In was used for the diagnostic arm as ^{111}In-DTPA-conjugated octreotide.[102]

Yet, following pilot studies with the positron emitter ^{86}Y,[103] ^{90}Y was utilized clinically for treatment as ^{90}Y-DOTA-TOC.[104] Later, ^{68}Ga was introduced for pre-therapeutic PET/CT.[105] In parallel, both new alpha-emitting trivalent radiometals such as ^{213}Bi and new positron emitters such as ^{44}Sc and ^{152}Tb were applied.[14d,106]

Since 2015, the identical theranostic concept is realized for prostate cancer, targeting the prostate specific membrane antigen (PSMA) with glutamate-urea-based targeting vectors. The first diagnostic version utilized the ^{68}Ga-specific chelator HBED, yet for THERANOSTIC purposes soon conjugated to DOTA derivatives such as e.g. DOTA-PSMA-617 were applied.[107] Again, ^{90}Y, ^{177}Lu and the alpha-emitters ^{213}Bi and, in particular promising, ^{225}Ac are therapeutic trivalent radionuclide[108] counterparts to ^{68}Ga. Recently, the potential of longer-lived ^{44}Sc (3.9 hours half-life) compared to short-lived ^{68}Ga (1.1 hours half-life) was demonstrated.[109]

Other examples covered by this strategy refer to gastrin-releasing peptide receptor antagonists,[110] chemokine receptor affine CXCR4-tracers[111] and other peptidic structures. Finally, also non-peptidic targeting vectors benefit from the THERANOSTIC strategy mentioned based on the principal design of radiotracers according to Figure 1. In particular, bisphosphonates conjugated to DOTA-derivatives are promising compounds for the treatments of disseminated bone metastases with ^{177}Lu or ^{225}Ac, following molecular imaging with ^{68}Ga-analogue tracers.[112]

5. DOTA in Unique Radiochemical Separations

5.1 Hot Atom Chemistry

5.1.1 Cold and Hot Atoms

Temperatures of atoms are cross-linked to their energies and to their average speed of movement. The energy for a certain state of a particle is $E_{kin} = 1/2mv^2$. This is quantitatively expressed by the Maxwell-Boltzmann correlation bridging speed, mass and temperature with probability density functions f(v), which quantity the probability of the particles speed per unit of speed, where the translational energy corresponds to a certain temperature. At room temperature, atoms or molecules move or "vibrate" within their bounds according to "thermal" energy. For the nitrogen gas N_2, "most probable" velocities are 422 m/s at "room" temperature, i.e. 26.85 °C = 300 K, and 688 m/s at 800 K (526.85 °C). Doubling the absolute temperature (Kelvin scale) increases this velocity by a factor of $\sqrt{2} \approx 1.4142$. (Those speed distributions, by definition, apply to ideal gases, where interactions between the atoms or molecules are zero. Real gases, of course, differ, and so do their speed distributions. In condensed matter, where many of the "hot" atom chemical reactions proceed, the situation is much more complex.

Historically, a "hot atom" connoted an atom "freshly" formed by a nuclear process – which could be a spontaneous transformation of an unstable, radioactive nuclide, but also the product of a nuclear reaction induced on a stable target nucleus. The term "hot atom chemistry" now is synonym for "chemical effects of nuclear transformations". According to the IUPAC, it is defined as "The rapture of the chemical bond between an atom and the molecule of which the atom is part, as a result of a nuclear reaction of that atom".[113]

In an abstract sense, "hot" means "higher temperature", and higher temperature means "higher energy". For a particle, "higher energy" means "higher velocity". As chemical effects are concerned, those "hot" atoms should own a translational or electronic energy above conventional chemical bond energies. Because of primary nuclear transformations of unstable nuclei or of nuclear reactions, the recoil atom with its corresponding impulse and kinetic energy can be attributed by an incredible quasi-temperature of the "hot" atom – yielding an estimation on the chemical "reactivity" of such an atom. Both aspects (translational or electronic energy) are the reason for a "rupture" of the chemical bonds the atom is/was involved in.

However, referring to either "translational" or "electronic" energy indicates that the chemical reasons of how "hot atoms" rupture chemical bonds may differ. The first aspect is related to the pure "speed" and/or energy of the atom. Chemically speaking, this refers to the primary effect of the recoil energy of the nucleus of an atom formed. The second aspect addresses the rapid and dramatic changes of the electron shell occupancies and structures within the shell of the atom, being inherent consequences of primary and secondary radioactive transformation processes (i.e. mainly induced by electron vacancies generated by positron emission or electron capture). The sciences of hot atom chemistry have been studied systematically in the 1960–1990s, and comprehensive books are collecting a variety of experimental data and theoretical concepts, such described in the book by Matsuura and Adloff et al.[114]

Recoil energies are well defined for α-, β-, IC- and γ-emissions. Basically, nuclear recoil follows the conservation of impulses, and impulses $p = mv$ and kinetic energies $E_{kin} = 1/2mv^2$ refer to two species formed in the primary or secondary nuclear transition. As larger the recoiling nucleus is, as lower is its kinetic energy. For the identical mass of a recoil nucleus, its kinetic energy is as larger as the mass and the energy of the second component is. Accordingly, recoil energies are large for α-emissions (reaching the 0.1 MeV level), lower for β-emissions, and lowest for photon-emission (eV scale).

Primary α-emissions: Already in 1904 it was realized that the α-transformation process gives the new nucleus a significant recoil energy – an effect measured in terms of its (chemical) separation from the parent radionuclide. The product nucleus appeared to be "volatile" relative to the parent nuclide fixed on the surface of a solid. For example, ^{214}Pb ($t_{1/2}$ = 26.8 min), the product of ^{218}Po ($t_{1/2}$ = 3.05 min) undergoing α-transformation, was radiochemically isolated "without" chemistry in 1904: "Since radium A breaks up with an expulsion of an α particle, some of the residual atoms constituting radium B, may acquire sufficient velocity to escape into the gas and are then transferred by diffusion to the walls of the vessel."[115] (Radium A = ^{218}Po, Radium B = ^{214}Pb). Using the same concept and further along the ^{226}Ra natural transformation chain (^{214}Pb $\rightarrow \alpha \rightarrow$ ^{210}Hg $\rightarrow \beta^- \rightarrow$ ^{210}Tl), ^{210}Tl ($t_{1/2}$ = 1.3 min) was isolated from that ^{214}Pb by Hahn and Meitner in 1909.

Primary β-emissions: The β-electrons are of relatively high maximum kinetic energy, reaching MeV scales. Due to their low mass, however, and because most of the β-particles emitted are of much lower kinetic energy than the E_{max} value (continuous β spectrum), the average recoil energy of the formed nucleus is small. Nevertheless, the nuclei formed in β-transformation processes are always chemically different from the initial element. Thus, in all cases the new element is a different one – and except for example in transitions between trivalent lanthanides of chemical properties significantly different from those of the progenitor. For example, a radioactive halogen atom may transform into a noble gas (β^-) or a group VI element (β^+ and EC); a divalent radioactive metal may transform into a trivalent- (β^-) or into a monovalent metal (β^+ and EC). In all cases, either covalent or coordination bounds are broken and changed into different ones. This is referred to as "post-effects" of nuclear transformations and has a significant impact on speciation chemistry and, in particular, separation chemistry.

Secondary γ-emissions: De-excitation of excited nuclear states (such as in transition processes of meta-stable nuclear isomers) the recoil energy is small (ca. 5 keV). This energy is generally too low to induce molecular rupture directly. This relates to most of the isomeric transitions.

5.1.2 Orbital Electron Capture and Cascades of Releasing Electrons and Filling Electron Vacancies

Auger cascades are synonymously with extreme ionization of the residual atom. Electrons initially involved in chemical bonds are lost. Moreover, the high positive charge of the residual atom is immediately spread to neighbor atoms of the same initial molecule, inducing a "coulomb explosion". Atomic and molecular fragments are formed, each with individual secondary recoil energy (depending on their mass). Finally, the high number Auger electrons emitted, though of relatively low kinetic energy, creates intense local ionization in condensed matter (cf. the LET values of the various particles). Local ionization is radiolysis of e.g. water, again causing rupture of chemical bonds. The electrons themselves are, at least in principle, able to oxidize surrounding atoms. A similar process occurs when refilling a vacancy in an inner electron shell caused by internal conversion or by positron emission.

5.1.3 Recoil Energies in Nuclear Reactions

When in 1934 Szilard and Chalmers bombarded C_2H_5I with neutrons causing a $^{127}I(n,\gamma)^{128}I$ nuclear reaction, they observed experimentally that, surprisingly, ca. 60 % of the ^{128}I activity detected were "inorganic" ^{128}I iodine, while the remaining ca. 40 % still were represent as $C_2H_5{}^{128}I$. In nuclear reactions, recoil energies depend on the type and energy of the projectile, the type of the ejectile and the mass of the product nucleus. For example, recoil energies are in the order of 0.1 keV for (n,γ) reactions and 0.1 MeV for (n,p) reactions. In terms of radiochemical separation, the effect is obvious: The fraction of "inorganic" ^{128}I (precipitated as $Ag^{128}I$) can be separated chemically from the "organic" $C_2H_5{}^{128}I$ and from the irradiated, non-radioactive target material $C_2H_5{}^{127}I$. This is a clear evidence of a hot atom chemistry way to isolate radioactive and nonradioactive isotopes of the same element. Szilard himself wondered that to "... separate the radioactive iodine from the bulk of bombarded iodine ... sounds blasphemic to the chemist...".[116] Consequently, an additional term was introduced for the option of using hot atoms for chemical separations: The Szilard/Chalmers reactions.[117]

An early assumption was that the momentum imparted on the iodine atom by the impinging neutron would rupture the C-I bond. However, this rupture can be observed also by low-energetic, thermal neutrons of ca. 0.02 eV energy - much too low to simply knockout the iodine atom. In the present context, it is not the direct effect of nucleus A displacement induced by the incoming projectile a of the nuclear reaction process of type A(a,b)B, what matters: it is the recoil of the radioactive product nucleus B caused by the ejectile b of the nuclear reaction – in the present case the photon of the (n,γ) process.

5.2 Two Elements: Radiochemical Separation of Neighbor Radio-Lanthanides

5.2.1 Hot Atom Effects Applied to Radiochemical Radioisotope Separation and Radioisotope Enrichment

One of the unique features of radiochemistry is its ability to separate two isotopes of the same chemical element in the course of radioactive transformation processes. This is exclusively due to hot atom effects, and is mostly related and applied to the production of relevant radionuclides in the course of neutron-capture nuclear reactions, mostly with thermal neutrons, i.e. $A(n_{th},\gamma)B$ reactions with A being a stable isotope A of a chemical element E ($_ZE_N$) and B being $_ZE_{N+1}$. In this case, the radioactive product B is isotopic with the target element A, and it cannot be separated chemically. Consequently, the product nucleus B co-exists with the target atom. Its specific activity is its absolute radioactivity related to the cumulative mass of B *and* A. Depending on the mass of A used, the neutron flux and the neutron capture cross-section, specific activities of B are relatively low, in particular at non-high flux reactors. Hot atom chemistry, however, allows isolating a certain fraction of the product radioisotope B from the target element.

There are different options of the fate of a radioisotope produced in a nuclear reaction illustrated for (n,γ) processes: A stable target nucleus chemically bound within a molecular or crystalline matrix (the "cage" as illustrated schematically in Figure 5 as a three-dimensional box with dotted lines indicating chemical bonds) is irradiated. Scenario 1 is thermalization of the hot atom nucleus and a terminal chemical stabilization as a new species. Scenario 2 is a process, where the hot atom "returns" to a vacancy created within the cage and finally remains there. Scenario 3 is a concept, where the hot atom hits a stable atom to eject it out from the cage to finally take over its position again within the cage. Both options 2 and 3 are called "retention" or "annealing reactions". In both cases, the radioisotope B finally finds itself the "cage", i.e. as the chemical species of the irradiated target material. Experimentally, it depends on the physico-chemical properties of this material (including metal-ligand complexes, oxides, salts etc.).

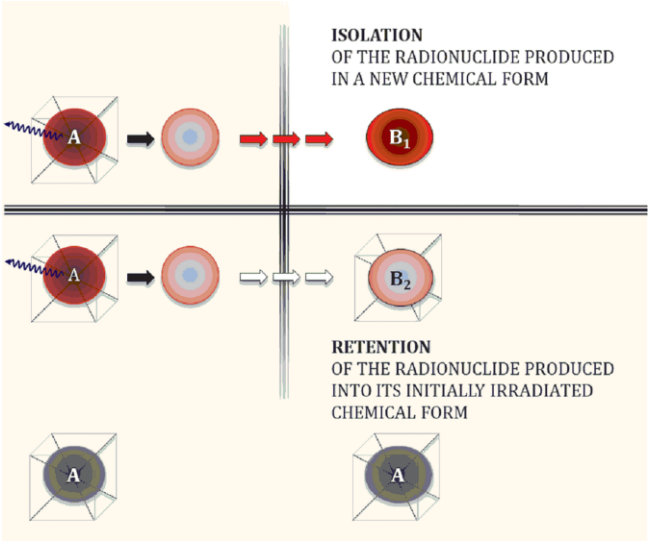

Figure 5. Concept of radiochemical separation of stable and radioactive isotopes of the same element in Szilard/Chalmers type processes.

The other option is B thermalizing as it is. Now, it terminates in a new chemical form, which is: outside the "cage". While those processes are ongoing continuously with the irradiation, the distribution of the different chemical species of B is fixed at the end of bombardment. Yet, the mechanistic explanation of the individual processes is quite complex and difficult. Clearly, there is a relevant recoil of ^{128}I determined by the ejected photon, which plays a major role. However, in addition, de-excitation of nuclear states in ^{128}I accompanied by internal conversion and Auger electron emissions contribute to coulomb and charge effects and ionizations. Nevertheless, the basic aspects are initial bond rupture, energy transfer, charge transfer, ionization, radical formation, and ultimate chemical speciation. This altogether influences the ^{128}I product distribution pattern. Anyhow, the formation of a new chemical species of the radioisotope produced is the essence of the separation of a radioisotope from a stable isotope of one and the same chemical element.

Based on the Szilard/Chalmers type processes the "fate" of a radioisotope produced in a nuclear reaction (stable A to radioactive B) is either to terminate as a new, chemically different chemical species (B_1) or to return into the initial species (B_2), where it is co-existing with an excess of the initial target compound containing the stable target nucleus isotope (A), which did not undergo any nuclear reaction. Radiochemical separation isolates the fraction of B_1 from both the inactive target material and the fraction B_2 of the radioisotope, which had returned into the cage. As lower the amount of stable A (2+3 in Figure 5) is in the isolated fraction of B, as higher its isotopic "enrichment" is and as larger is the increase in the final specific activity of that fraction of B isolated. In laboratory experiments, enrichment factors of 1000 and more have been reported. In large-scale isotope productions, however, this is somewhat lower because of many reasons. The main factor is the simultaneous decomposition of the chemical bonds of the target material itself due to the high ionization density caused by the irradiation, yielding a spectrum of species fragments. Consequently, enrichment factors are as higher as lower the neutron flux is and as shorter the irradiation period. Table 5 lists some typical studies, where nuclear reaction radioisotope products have been "enriched" in terms of specific activity.

The key factor to achieve maximum enrichment lies in the stabilization of the hot atom B in a defined chemical environment and to block the backward transfer of B into the cage. A conclusive example is the enrichment of a radiolanthanide isotope produced by thermal neutron capture as produced from an isotopic, macroscopic lanthanide target. Both A and B are isotopes of one and the same chemical element, and both A and B are trivalent lanthanides of identical chemistry.

Proof-of-principle nuclear reaction: ^{165}Ho(n,γ)^{166}Ho. The concept is to use a target material of type metal-ligand ML complex, with L representing a macrocyclic chelate such as DOTA. Complexes of type [Ln(DOTA)]$^-$ (Figure 6) are extremely stable, both in terms of thermodynamic and kinetic aspects, as already discussed in Section 2. These complexes are formed only at elevated temperature (close to 100 °C). So if the "hot" radiolanthanide created in the course of the nuclear reaction is released from the irradiated complex (and this is typically at room temperature), it will not form a DOTA complex again: The "hot" ^{166}Ho thermalizes as a ^{166}Ho^{III} cation. Consequently, it can be separated from the intact [^{165}Ho(DOTA)]$^-$ target species (Figure 7). This combines unique thermodynamic and kinetic parameters of [Ln(DOTA)]$^-$ complexes with the hot atom chemistry

Table 5. Representative examples of isotope enrichments due to Szilard/Chalmers type hot atom chemistry separations. Experimental examples from Ebihara and Collins 1984.[118].

*B	σ A(n,γ) (barn)	$t_{1/2}$ *B	Target A species	Product *B species	Separation chemistry	Separation yield [%]	Enrichment factor
^{51}Cr	15	27.7 d	$KCrO_4$	$^{51}Cr^{III}$	$Cr(OH)_3$ co-precipitation or adsorption	8–10	500–10000
^{59}Fe	1.3	44.50 d	[K] ferrocyanide	$^{59}Fe^{III}$	Cation exchange	40	400
^{55}Fe	2.3	2.73 a					
^{64}Cu	4.5	12.70 h	[K] ferrocyanide	$^{64}Cu^{II}$	Cation exchange	55–94	1000–2500
^{65}Zn	0.74	244.3 d	Zn phthalo-cyanide or ferrocyanide	$^{65}Zn^{II}$	Cation exchange	45	500
^{76}As	4.0	26.4 h	Triphenyl arsine or cacodylic acid	$^{76}As^{III}$	$As(OH)_3$ co-precipitation with $Fe(OH)_3$ or extraction of arsenate in water	35	800

of radionuclides following nuclear reactions. Within this experimental design, enrichment factors at the TRIGA research reactor Mainz of 1000 have been observed.

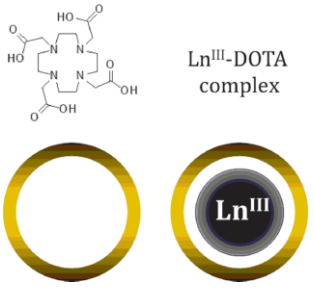

Figure 6. Left: the macrocyclic ligand DOTA as chemical structure and pictogram. Right: A trivalent lanthanide [Ln(DOTA)]$^-$ complex pictogram.

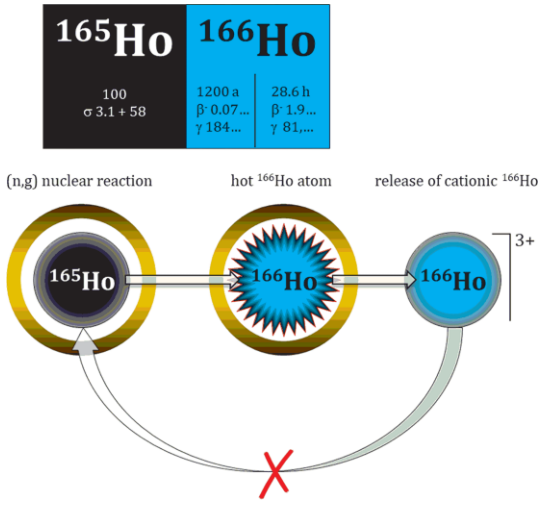

Figure 7. Radiochemical separation of the "hot" $^{166}Ho^{III}$ cation from neutron-irradiated ^{165}Ho(DOTA) targets.[119]

5.3 One Element – Two Isotopes: Radiochemical Separation of a Lanthanide Radioisotope from its Stable Isotope

The physico-chemical processes occurring after the primary radioactive decay, such as electron capture (EC) and/or Auger electron emission or X-ray emission, care known to provide the possibility to separate of different chemical forms of the parent and daughter radionuclides.[120]

This particular kind of radiochemical separation utilizes the effects of post-processes subsequent to a radioactive transformation process of an unstable nuclide *K1 → *K2. It is a consequence of the processes within the electron shell of *K2. Attempts to separate neighboring lanthanides have been reported for several cases as well. A prototype of continuous separation (a radionuclide generator system) of type $_Z{}^A$Ln/$_{Z-1}{}^A$Ln was reported for the ^{140}Nd ($t_{1/2}$ = 3.37 d)/^{140}Pr ($t_{1/2}$ = 3.4 min) pair. The daughter ^{140}Pr is formed via electron capture transformation of ^{140}Nd. This ^{140}Pr ($_{Z-1}{}^A$Ln) is released from the chemical microenvironment of the ^{140}Nd ($_Z{}^A$Ln)-DOTA complex. Thus, the fraction of "free" $^{140}Pr^{III}$, i.e. non [^{140}Pr(DOTA)]$^-$, can be effectively separated from the [^{140}Nd(DOTA)]$^-$ complex for the concept (Figure 8).

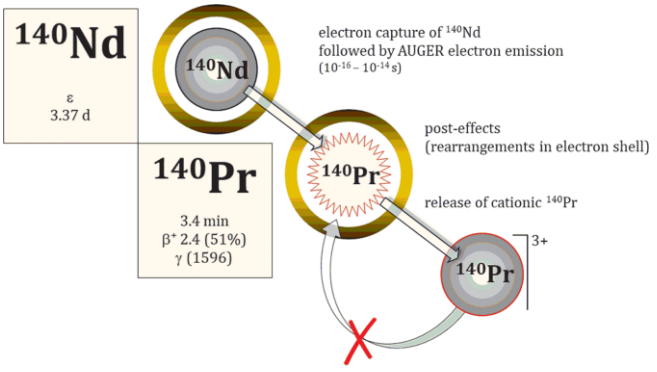

Figure 8. Concept of radiochemical separation of two radioactive isotopes of chemically almost identical elements in Szilard/Chalmers type processes: the $^{140}Pr^{III}$ cation generated via the primary β^+-process from neutron-deficient ^{140}Nd coordinatively bound in a DOTA complex, and the "fate" of the hot ^{140}Pr atom.[121]

This combines unique thermodynamic and kinetic parameters of [Ln(DOTA)]$^-$ complexes with the hot atom chemistry of radionuclides following nuclear transformations.

There are different options to realize the ^{140}Nd/^{140}Pr separations, which all start with the synthesis of a [^{140}Nd(DOTA)]$^-$ complex or a ^{140}Nd(DOTA)-conjugated compound with particular chemical features derived from the two different species. In a first version of a radiochemical separation, ^{140}Pr is isolated from [^{140}Nd(DOTA)]$^-$ by means of cation exchange chromatography. The mixture of [^{140}Nd(DOTA)]$^-$ + ^{140}Pr is eluted through a strong cation exchanger resin, which selectively adsorbs the $^{140}Pr^{III}$ cation. The [^{140}Nd(DOTA)]$^-$ complex, in contrast, passes the cartridge (Figure 9). This approach is, however, not an applicable radionuclide generator design, as the generator parent nuclide is mobilized rather than immobilized. A "real" ^{140}Nd/^{140}Pr radionuclide generator system is achieved, for example, by adsorbing the parent radionuclide ^{140}Nd in form of a ^{140}Nd(DOTA)-

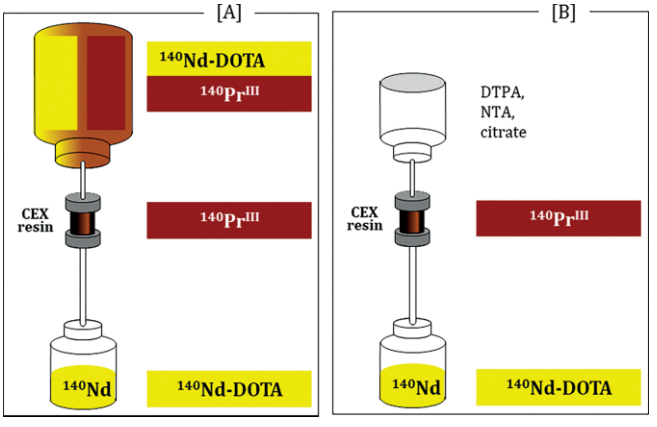

Figure 9. ^{140}Pr as isolated from [^{140}Nd(DOTA)]$^-$. [**A**] Eluting a mixture of [^{140}Nd(DOTA)]$^-$ and $^{140}Pr^{III}$ through a cation exchange resin. The cartridge selectively adsorbs the $^{140}Pr^{3+}$ cation. The [^{140}Nd(DOTA)]$^-$ complex is not absorbed, collected in a vial and starts to generate the ^{140}Pr generator daughter again. [**B**] Subsequently, the $^{140}Pr^{III}$ cation adsorbed on the resin is desorbed using adequate aqueous solvents such as HCl or ligand L solutions (e.g. DTPA, NTA, citrate etc.), forming ^{140}PrL complexes.[121]

conjugated compound such as ^{140}Nd(DOTA)-TOC. (TOC represents the peptide DPhe^{1}-Tyr^{3}-octreotide in Scheme 2).

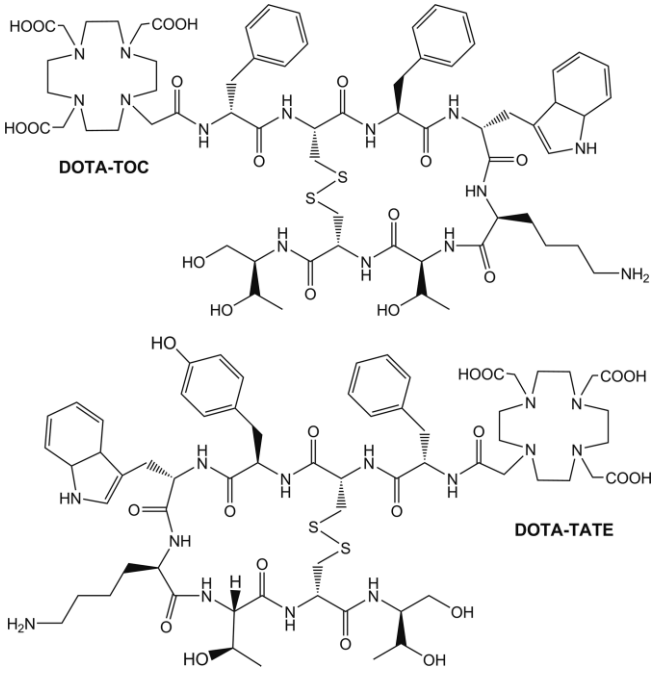

Scheme 2. Chemical structures of DOTA-TOC and DOTA-TATE.

DOTA-TOC represents a DOTA-conjugated peptidic targeting vector addressing the somatostatin receptor, overexpressed on the extracellular surface of neuroendocrine tumors. It is one of the key compounds used to synthesize radiopharmaceuticals for molecular imaging (utilizing the trivalent positron emitter ^{68}Ga or the trivalent single photon emitter ^{111}In), but also for the treatment of those tumors (utilizing trivalent beta emitters such as ^{90}Y or ^{177}Lu as well as trivalent α-emitters such as ^{213}Bi and ^{225}Ac). The peptidic part of this compound guaranties for strong adsorption on surfaces of adequate solid phases (such as on selected resins/cartridges). The transformation product ^{140}Pr generated, if present in a cationic form, can be removed from this solid phase. An approach of chemically stable binding of ^{140}Nd(DOTA-TOC) species on a stationary solid phase (C-18) with subsequent elution of the ^{140}Pr released in an aqueous phase was demonstrated in Figure 10.[121]

While the ^{140}Nd remains chemically fixed at the ^{140}Nd position (because of the stability of the [^{140}Nd(DOTA)]$^{-}$ coordination bonds and the stable adsorption of the peptidic part of the ^{140}Nd(DOTA-TOC)), the effective isolation of ^{140}Pr depends on the composition of the aqueous medium. The challenge is to provide a chemical environment, which rapidly stabilize the hot ^{140}Pr created in a cationic or complex form easily to separate. DTPA, NTA (H_3NTA = nitrilo-triacetic acid) and citrate are ligands known to rapidly form stable Ln^{III} complexes with thermodynamic stability constants (lg K_{LnL}) of log $K_{Pr(DTPA)}$ = 21.07,[122] log $K_{Pr(NTA)}$ = 10.88 and log $K_{Pr(NTA)2}$ = 8.18,[123] log $K_{Pr(citrate)}$ = 8.72 and log $K_{Pr(citrate)2}$ = 3.88.[124] The elution yield of ^{140}Pr in DTPA, citrate and NTA solutions is presented in Figure 11 as a function of the ligand concentration: about 20 % of ^{140}Pr^{III} generated could be eluted with 1 mL of pure water. In

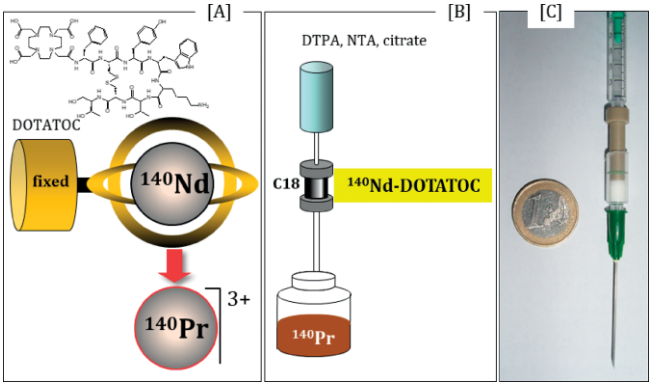

Figure 10. A simplified illustration of ^{140}Nd/^{140}Pr radionuclide generator concepts: [**A**] ^{140}Nd(DOTA-TOC) (TOC being an octapeptide binding to reverse-phase C18 resins), with ^{140}Pr being generated. [**B**] Fixing ^{140}Nd(DOTA-TOC) on a C18 cartridge and exclusively eluting from that cartridge the ^{140}Pr^{III} species generated. [**C**] Photo of the simple experimental design of the middle concept. The generator column could be operated with standard single-used syringes. Elution with 1 mL of the eluate.

contrast, > 93 % of the ^{140}Pr activity could be obtained in 1 mL of 10^{-3} M DTPA eluate. (The elution yield decreased with decreasing ligand concentration and was around 20 % at a concentration ≤ 10^{-4} M DTPA.) The elution capacity of citrate and NTA was evidently poorer: about 90 % of ^{140}Pr could be eluted only at 0.1 M concentration of citrate and NTA solutions. This obviously is due to lower complex stability of the trivalent Pr^{III} with citrate and NTA ligands (Figure 11).[121]

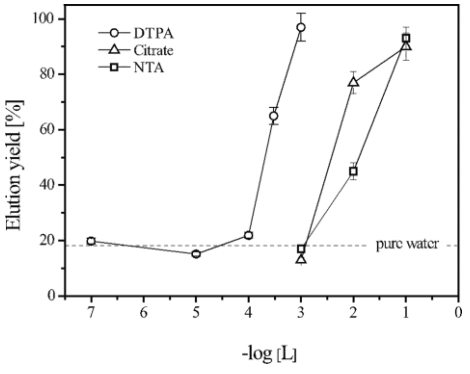

Figure 11. Elution yield of ^{140}Pr in 1 mL of aqueous solutions of various ligands L relative to elutions with pure water as a function of ligand L concentration. ([DTPA] = 10^{-7} – 10^{-3} M, [citrate] = 10^{-3} – 10^{-1}, [NTA] = 10^{-3} M, pH < 6).[121]

At an actual ^{140}Nd activity of about 100 MBq and 0.5 h time lapse after the last elution (time enough for accumulation of ^{140}Pr saturation activity), the breakthrough of ^{140}Nd is about 25 kBq only (ca. 0.025 %). The hot atom chemistry-based generator design thus shows high elution yield and extremely high chemical and radiochemical efficacy – despite the almost identical chemistry of the two neighbor lanthanides. It combines hot-atom chemistry, in particular post-effects of nuclear transformation, with chemical consequences relevant for lanthanide speciation. Together with the adequate thermodynamic and kinetic inertness of the macrocyclic chelator DOTA, the concept allows efficient radiochemical separations.[121,125]

5.4 One Element – One Isotope – Different Nuclear States: Chemical Separation of Ground-State and Excited Nuclear Isomers

The ultimate challenge in radiochemical separation strategy is to discriminate between two nuclear states of one and the same isotope. The separation of the meta-stable nuclear requires that the de-excitation of the excited nuclear state towards the ground state proceeds in a way that chemical (covalent or coordinative) bonds the metastable isotope initially had in its chemical species are disrupted. The new nuclear level (in most cases the ground state isomer) then is formed as a new chemical species, which may be separated radiochemically from the initial species.

Obviously, this effect requires a detailed look on the transition pathways the excited nuclear levels undergoes. There are several options; in particular, in the case the ground state of the isotope in question is not representing a stable nucleus. In this case, the first option is a primary transformation (typically β-transformation processes or α-transformation) from the meta-stable nuclear isomer not to its ground state but approaching the next nucleus with higher mean nuclear binding energy. For "inner" transitions between the two nuclear isomers, there are three options; emission of electromagnetic radiation (photons, γ-rays), internal conversion and/or pair formation.[126]

Rupture of chemical bounds the metastable isomer initially would require either a significant energy released in those transitions, including recoil energies. Those energies are typically not sufficiently high to induce chemical effects. Alternatively, there are post-effects, which immediately affect the electron shell of the atom of the nuclear isomer. Of particular interest is the pathway of inner conversion. Here, the difference in energy ΔE between the metastable and ground state levels of the same nucleus is utilized to release an s-orbital electron, mainly from the K-shell, but also from L and M shells. This vacancy in the electron shell needs reorganization, and two processes compete for it: emission of electromagnetic radiation (fluorescence, i.e. X-rays) and emission of Auger and Coster-Kronig shell electrons. It is the later one, which finally creates a highly positively charged cation as an intermediate. Thereby, existing chemical bounds of that atom are broken. In condensed matter, the highly charged atom immediately reorganizes its electron shell according to the proton number of the nucleus. This reorganization may form chemical species different to the chemical bonds the "gone" metastable isomer initially had. In this situation, two chemically different species may exist simultaneously: the initial one with the meta-stable isomer, and a new one with the ground-state isomer. Obviously, those species may be separated chemically.

There are only very view reports on this kind of separations. Recently, there have been publications on two different cases, where again trivalent radiometals are involved. Indeed, the fate of meta-stable states $^{m}M^{III}$ in the form of initial $[^{m}M(DOTA)]^{-}$ complexes have been studied; i.e. resembling the situation illustrated for ^{140}Nd(DOTA)-compounds vs. the ^{140}Pr-Pr^{3+} cation generated following the β^{+}-transformation of the ^{140}Nd parent nucleus to the ^{140}Pr daughter nucleus. Similarly, the meta-stable nuclear "parent" state would remain as $[^{m}M(DOTA)]^{-}$ complex, while the ground-state "daughter" ^{g}M would exist as single cation $^{g}M^{3+}$.

One experimental study refers to the pair ^{177m}Lu/^{177g}Lu, with ^{177m}Lu being the long-lived metastable nuclear isomer ($t_{1/2}$ = 160.4 d) and ^{177g}Lu representing the ground state ($t_{1/2}$ = 6.61 d), see Figure 12 left). The other system is ^{44m}Sc ($t_{1/2}$ = 2.44 d) and ^{44g}Sc ($t_{1/2}$ = 3.92 h, see Figure 12 right). For the pair ^{177m}Lu/^{177g}Lu the aim was to verify that the ground state ^{177g}Lu can be separated radiochemically from the meta-stable one present as an ^{177m}Lu(DOTA) species.[127] In this context, the separation of two nuclear isomers with the meta-stable one representing the longer-lived, the pairs would represent radionuclide generators.

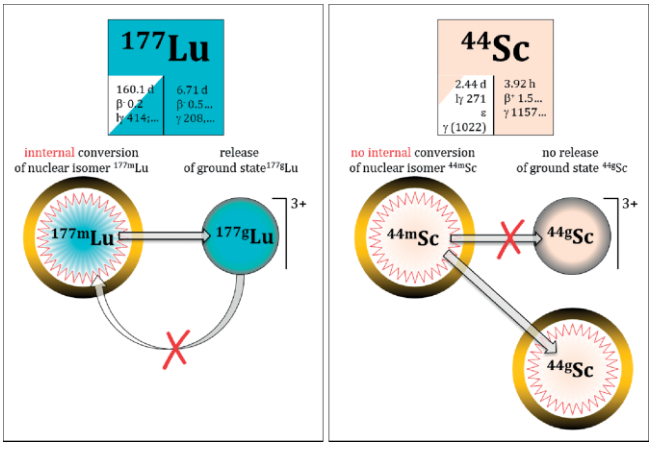

Figure 12. Radiolanthanide-DOTA species studied for the pairs ^{177m}Lu/^{177g}Lu and ^{44m}Sc/^{44g}Sc.

For the pair ^{44m}Sc/^{44g}Sc, in contrast, the aim was to demonstrate that the ground state is not released from the initial ^{44m}Sc species, thereby forming a stable in vivo generator.[128] If of interest for nuclear medicine, some of those pairs "in vivo generators" are discussed in literature.[129]

^{177m}Lu/^{177g}Lu: ^{177g}Lu is of great interest in endoradiotherapy and is produced either by neutron capture reaction on ^{176}Lu or on ^{176}Yb. The first pathway coproduces the long-lived metastable ^{177m}Lu with ca. 0.02 % relative to ^{177g}Lu at EOB. The pathway starting from ^{176}Yb produces ^{177}Yb, which transfers via β^{-} transformation to the ^{177g}Lu ground state exclusively. In addition to this radionuclide purity that ^{177}Lu can also be separated from the irradiated ^{176}Yb target material,[130] providing extremely high specific activity. The difference ΔE between meta- and ground state of ^{177}Lu is 970.18 keV.[131] While 78.6 % of the transformations proceed via the β^{-} process to ^{177}Hf states, ^{177m}Lu utilizes 21.4 % of its transformation to approach ^{177g}Lu mainly via internal conversion. The ^{177m}Lu internal conversion coefficient ICC is 30.7 (ICC = internal conversion coefficient).[127] As illustrated in Figure 12, this internal conversion induces post-processes in the electron shell of the ground state formed. Starting from the ^{177m}Lu(DOTA) species ^{177m}Lu(DOTA-(Tyr^{3})-octreotate) (DOTA-TATE), an analogue of DOTA-TOC (Scheme 2), a significant fraction of ^{177g}Lu is detected as cationic species and can chemically be separated. The authors observe effects concerning the temperature of the system and its impact on the ^{177g}Lu accumulation rate. The study concludes

that the transition pathways of ^{177m}Lu and an efficient separation chemistry may allow to produce radionuclidic pure ^{177g}Lu from mixtures of ^{177m,g}Lu or ^{177m}Lu itself.

^{44m}Sc/^{44g}Sc: ^{44}Sc has attracted interest as a trivalent metallic positron emitter, analogous to ^{68}Ga, due to its longer half-life. It was initially made available via the ^{44}Ti/^{44}Sc radionuclide generator.[14d,132] This pathway produces the ground state exclusively. In parallel, there are attempts to produce ^{44}Sc directly at cyclotrons. One option is the ^{44}Ca(d,n)^{44}Sc process. In this process, however, the metastable ^{44m}Sc is coproduced.[133]

One of the interesting studies related to the clinical application of ^{44}Sc for PET/CT molecular imaging is, whether that long-lived metastable ^{44m}Sc could be utilized as an in vivo generator. The concept is (1.) to label a radiopharmaceutical with the long-lived parent of the relevant radionuclide, to (2.) let the radiopharmaceutical distribute in vivo until accumulation at the desired target site is achieved, and (3.) detect the radiation emitted from the nuclide *generated*. This concept, however, would require that the generated ground-state "daughter" nuclide be not released from the radiopharmaceutical labelled with the meta-stable "parent" radionuclide. Specifically, for the potential in vivo generator pair the challenge would be to identify a chelate-conjugated radiopharmaceutical, where the ^{44m}Sc-chelate complex would not release the ^{44g}Sc generated in vivo.

The difference ΔE between meta- and ground state of ^{44}Sc is 271 keV. ^{44m}Sc undergoes a primary transformation (β^+, 1.2 % abundance) to ^{44}Ca. Inner transition from ^{44m}Sc to ^{44g}Sc thus is highly abundant (98.8 %). However, different to the situation introduced for ^{177}Lu, this amount of ΔE = 271 keV is dominantly released as γ-emission. The internal conversion coefficient is ICC = 0.1391 compared to ICC = 30.7 for ^{177m}Lu. The recoil energy associated with this emission is estimated to amount 0.89 eV – much too small to induce changes in electron bonds (bond strengths in the DOTA chelator are given as 3 eV),[129d] Inner conversion is almost negligibly with 2.74 % abundance only. Accordingly, there are only small effects related to changes in the electron shell. Experimentally, this was demonstrated measuring the release of ^{44g}Sc from ^{44m}Sc(DOTA-TATE) species – which is negligible.[134]

This indeed makes a difference compared to the pair ^{140}Nd/^{140}Pr, see above, where the short-lived daughter nucleus ^{140}Pr is released following electron capture transformation of ^{140}Nd and is released from e.g. ^{140}Nd-DOTA compounds. In order to avoid the release of ^{140}Pr to design an in vivo generator for this pair should try to use open-chain chelators such as e.g. DTPA derivatives instead of DOTA.[135]

6 Conclusion: Chemical Immobilization vs. Nuclear Mobilization

Introduced to molecular imaging as lanthanide(III)-DOTA moiety in contrast agents for MRI, and subsequently transferred to radiopharmaceutical chemistry and nuclear medicine, the macrocyclic chelator DOTA offers extraordinary features in terms of both thermodynamic and kinetic stability of [M(DOTA)]$^-$ complexes.

Efficient complex formation with trivalent radiometals such as ^{68}Ga, ^{44}Sc, ^{90}Y, ^{177}Lu and other radiolanthanides, ^{213}Bi, ^{225}Ac etc. requires temperatures close to 100 °C, but ones the trivalent radiometal terminated inside the DOTA core, it will remain there "forever" under room temperature (or human body temperature). This kinetic inertness is a key moment for the application of M-DOTA-conjugated radiopharmaceuticals. Accordingly, [M(DOTA)]$^-$ complexes remain extremely stable chemically under neutral pH and room temperature conditions without chemical dissociation. However, the nuclear transformation of a certain radiometal M may induce a kind of radiative dissociation of the initial M(i)-DOTA species. Interestingly, the new and final radiometal M(f) species formed following the nuclear transformation from M(i) to M(n) is unable to "return" into a M(f)-DOTA complex again at room temperature.

This article summarized promising applications of DOTA beyond nuclear medicine applications: rapid radiochemical separations induced by nuclear processes such as transformations of an unstable nuclide or radioisotope production in nuclear reactions. This behavior of [M(DOTA)]$^-$ complexes opens access to unique radiochemical separation strategies. Accordingly, DOTA assists radiochemical separations in cases, which for decades appeared to be impossible not only within conventional chemistry, but also within modern radiochemistry.

There are three groups of M(i) to M(f) nuclear transformations and transitions, which may benefit from the DOTA-assisted processes:

i) Separation of two chemically very similar elements:

Example: Radiochemical separation of two neighbor radiolanthanides,

ii) Separation of two chemically identic isotopes of the same chemical element:

Example: Radiochemical separation of a radioisotope produced in neutron capture nuclear reaction processes from its stable (nuclear reaction target) isotope

iii) Separation of two different nuclear states of the same isotope of one element:

Example: Radiochemical separation of ground-state isomer from an excited nuclear isomer with an option to chemically design a radionuclide generator system.

Those three options are summarized in Table 6. Black boxes in Table 6 highlight the examples, which have been discussed in this paper. More pairs are listed, which may be treated in a similar way. In the case of type *i*) separations, i.e. the separation of two chemically very similar elements neighbor radiolanthanides, the initial radiometal undergoes electron capture transformation. The rupture of chemical bonds associated with the re-formation of the electron shell of M(f) should release the new radiometal from the DOTA complex. Interestingly, some of the examples given may function as radionuclide generators (indicated by grey boxes), i.e. in cases where the half-life of M(n) is longer than that of M(f).

The potential of the chelator DOTA and its complexes with various metal species to be separated perfectly follows the statement given by Leo Szilard and T. A. Chalmers for the case of a *"Chemical separation of the radioactive element from its bombarded isotope in the Fermi effect"* in 1934: *"Whether the atoms freed (•••) will interchange with their isotopes bound in the irradiated chemical compound will depend on the nature of the*

Table 6. Possible nuclear transformations and transitions of type M(i) to M(f) which may result in a radiative dissociation of M(i)-DOTA complexes a mobilization of the M(f) species. For radioactive nuclides, the half-live is given. Black boxes highlight the examples, which have been discussed in this paper. More pairs to be separated are listed, which may be treated in a similar way.

Separation of:	M(i)	M(f)
Two elements	Radiochemical separation of neighbour radiolanthanides	
	^{140}Nd (3.37 d)	^{140}Pr (3.4 min)
	^{142}Sm (72.4 min)	^{142}Pr (40.5 s)
	^{146}Gd (48.3 d)	^{146}Eu (4.51 d)
	^{153}Tb (2.34 d)	^{153}Gd (239.47 d)
	^{158}Er (2.25 h)	^{158}Ho (21.3 min)
	^{160}Er (28.6 h)	^{160}Ho (26.8 h)
	^{161}Er (3.24 h)	^{161}Ho (2.5 h)
	^{163}Tm (1.81 h)	^{163}Er (75 min)
	^{165}Tm (30.06 h)	^{165}Er (10.3 h)
	^{166}Yb (56.7 h)	^{166}Tm (7.70 h)
In the case of the separation of two chemically very similar neighbour radiolanthanides, some of the examples given may function as radionuclide generators (indicated by grey boxes), i.e. in cases, where the half-life of M(n) is longer than that of M(f).		
One element – two isotopes	Radiochemical separation of a radioisotope from its stable isotope: the neutron capture production process and the isolation of a nuclear reaction product of high specific activity*	
	^{165}Ho	^{166}Ho (26.8 h)
	^{45}Sc	^{46}Sc (83.82 d)
	^{58}Fe	^{59}Fe (44.5 d)
	^{63}Cu	^{64}Cu (12.7 h)
	^{71}Ga	^{72}Ga (14.1 h)
	^{89}Y	^{90}Y (64.1 h)
	^{113}In	^{114m}In (49.5 d)
	^{139}La	^{140}La (40.25 h)
	^{140}Ce	^{141}Ce (32.5 d)
	^{142}Ce	^{143}Ce (33.0 h)
	^{141}Pr	^{142}Pr (19.13 h)
	^{146}Nd	^{147}Nd (10.98 d)
	^{152}Sm	^{153}Sm (46.27 h)
	^{158}Gd	^{159}Gd (18.49 h)
	^{159}Tb	^{160}Tb (72.3 d)
	^{164}Dy	^{165}Dy (2.35 h)
	^{164}Dy	^{166}Dy# (81.5 h)
	^{168}Er	^{169}Er (9.40 d)
	^{170}Er	^{171}Er (7.52 h)
	^{169}Tm	^{170}Tm (128.6 h)
	^{174}Yb	^{175}Yb (4.2 d)
	^{176}Lu	^{177}Lu (6.71 d)
*Mostly nuclear reaction products of relatively short half-life should be candidates to consider, because in this case irradiation periods would be relatively short, cf. Zhernosekov et al.[119] Those are given in grey boxes. # double neutron capture		
One element – one isotope – different nuclear states	Chemical separation of ground-state and excited nuclear isomers	
	^{44m}Sc (2.44 d)	^{44g}Sc (3.92 h)
	^{177m}Lu (160 d)	^{177g}Lu (6.71 d)
	^{154m}Tb (23 h / 9.0 h)	^{154g}Tb (21 h)
	^{158m}Ho (1 min / 27 min)	^{158g}Ho (11 min)
	^{162m}Ho (5.0 h)	^{162g}Ho (26 min)
	^{174m}Lu (142 d)	^{174g}Lu (3.31 a)
	^{86m}Y (48 min)	^{86g}Y (14.74 h)
	^{87m}Y (13 h)	^{87g}Y (80.3 h)
In the case of the separation of two nuclear states, some of the examples given may function as radionuclide generators (indicated by grey boxes), i.e. in cases, where the half-life of M(n) is longer than that of M(f).		

chemical compound with which we have to deal. If we work under conditions in which such an interchange does not take place, we obtain the radioactive isotope 'free', and by separating the 'free' element from the compound we can obtain any desirable concentration of the radioactive isotope."[117] However, the individual radiochemical separation must be investigated in detail. Both the immobilization of a M(i)-DOTA species and the mobilization of the cationic M(f) species are essential and may be arranged in different chemistries depending on a number of parameters.

Acknowledgments

G. T. is grateful for the support arriving form the Hungarian National Research, Development and Innovation Office (NKFIH K-120224 and K-128201 projects) and for the scholarship supported by the ÚNKP18-4 New National Excellence Program of the Ministry of Human Capacities. The research was also supported in a part by the EU and co-financed by the European Regional Development Fund under the project GINOP-2.3.2-15-2016-00008. F. R. wishes to thank K. P. Zhernosekov and D. V. Filosofov for the experimental studies on the ^{140}Nd/Pr and $^{165/166}$Ho examples. Open access funding enabled and organized by Projekt DEAL.

Keywords: DOTA · Thermodynamics · Kinetics · Radiolanthanides · Chemical separation · Hot atom chemistry

[1] a) E. W. Price, C. Orvig, *Chem. Soc. Rev.* **2014**, *43*, 260–290; b) M. I. Tsionou, C. E. Knapp, C. A. Foley, C. R. Munteanu, A. Cakebread, C. Imberti, T. R. Eykyn, J. D. Young, B. M. Paterson, P. J. Blower, M. T. Ma, *RSC Adv.* **2017**, *7*, 49586–49599; c) F. Roesch, P. J. Riss, *Curr. Top. Med. Chem.* **2010**, *10*, 1633–1668; d) T. J. Wadas, E. H. Wong, G. R. Weisman, C. J. Anderson, *Chem. Rev.* **2010**, *110*, 2858–2902; e) C. F. Ramogida, C. Orvig, *Chem. Commun.* **2013**, *49*, 4720–4739; f) L. Dai, C. M. Jones, W. T. K. Chan, T. A. Pham, X. Ling, E. M. Gale, N. J. Rotile, W. C. Tai, C. J. Anderson, P. Caravan, G. L. Law, *Nat. Commun.* **2018**, *9*, 857; g) M. W. Brechbiel, *Q. J. Nucl. Med. Mol. Imag.* **2008**, *52*, 166–173; h) E. Boros, A. B. Packard, *Chem. Rev.* **2019**, *119*, 870–901; i) C. S. Cutler, H. M. Hennkens, N. Sisay, S. Huclier-Markai, S. S. Jurisson, *Chem. Rev.* **2013**, *113*, 858–883; j) T. I. Kostelnik, C. Orvig, *Chem. Rev.* **2019**, *119*, 902–956; k) J. N. Liu, W. Bu, J. Shi, *Chem. Rev.* **2017**, *117*, 6160–6224; l) B. Bertrand, P. E. Doulain, C. Goze, E. Bodio, *Dalton Trans.* **2016**, *45*, 13005–13011.
[2] S. Hajela, M. Botta, S. Giraudo, J. Xu, K. N. Raymond, S. Aime, *J. Am. Chem. Soc.* **2000**, *122*, 11228–11229.
[3] a) A. Bianchi, L. Calabi, C. Giorgi, P. Losi, P. Mariani, P. Paoli, P. Rossi, B. Valtancoli, M. Virtuani, *J. Chem. Soc., Dalton Trans.* **2000**, 697–705; b) R. Delgado, J. J. da Silva, *Talanta* **1982**, *29*, 815–822.
[4] R. Delgado, J. Costa, K. P. Guerra, L. M. P. Lima, *Pure Appl. Chem.* **2005**, *77*, 569–579.
[5] E. Csajbok, Z. Baranyai, I. Banyai, E. Brucher, R. Kiraly, A. Muller-Fahrnow, J. Platzek, B. Raduchel, M. Schafer, *Inorg. Chem.* **2003**, *42*, 2342–2349.
[6] T. Fodor, I. Banyai, A. Benyei, C. Platas-Iglesias, M. Purgel, G. L. Horvath, L. Zekany, G. Tircso, I. Toth, *Inorg. Chem.* **2015**, *54*, 5426–5437.
[7] L. Burai, I. Fábián, R. Király, E. Szilágyi, E. Brücher, *J. Chem. Soc., Dalton Trans.* **1998**, 243–248.
[8] A. Takacs, R. Napolitano, M. Purgel, A. C. Benyei, L. Zekany, E. Brucher, I. Toth, Z. Baranyai, S. Aime, *Inorg. Chem.* **2014**, *53*, 2858–2872.
[9] A. Majkowska-Pilip, A. Bilewicz, *J. Inorg. Biochem.* **2011**, *105*, 313–320.
[10] Z. Baranyai, Z. Palinkas, F. Uggeri, E. Brucher, *Eur. J. Inorg. Chem.* **2010**, *2010*, 1948–1956.
[11] H. Irving, H. Rossotti, *Acta Chem. Scand.* **1956**, *10*, 72–93.
[12] G. R. Choppin, *J. Less-Common Met.* **1985**, *112*, 193–205.
[13] A. S. Merbach, L. Helm, É. Tóth, *The Chemistry of Contrast Agents in Medical Magnetic Resonance Imaging*, Wiley, **2013**.
[14] a) A. Rodriguez-Rodriguez, D. Esteban-Gomez, R. Tripier, G. Tircso, Z. Garda, I. Toth, A. de Blas, T. Rodriguez-Blas, C. Platas-Iglesias, *J. Am. Chem. Soc.* **2014**, *136*, 17954–17957; b) M. Perez-Malo, G. Szabo, E. Eppard, A. Vagner, E. Brucher, I. Toth, A. Maiocchi, E. H. Suh, Z. Kovacs, Z. Baranyai,

F. Rosch, *Inorg. Chem.* **2018**, *57*, 6107–6117; c) I. Velikyan, G. J. Beyer, B. Langstrom, *Bioconjugate Chem.* **2004**, *15*, 554–560; d) M. Pruszynski, A. Majkowska-Pilip, N. S. Loktionova, E. Eppard, F. Roesch, *Appl. Radiat. Isot.* **2012**, *70*, 974–979.
[15] É. Tóth, E. Brücher, I. Lázár, I. Tóth, *Inorg. Chem.* **1994**, *33*, 4070–4076.
[16] V. Comblin, D. Gilsoul, M. Hermann, V. Humblet, V. Jacques, M. Mesbahi, C. Sauvage, J. F. Desreux, *Coord. Chem. Rev.* **1999**, *185–186*, 451–470.
[17] X. Wang, T. Jin, V. Comblin, A. Lopez-Mut, E. Merciny, J. F. Desreux, *Inorg. Chem.* **1992**, *31*, 1095–1099.
[18] S. Aime, P. L. Anelli, M. Botta, F. Fedeli, M. Grandi, P. Paoli, F. Uggeri, *Inorg. Chem.* **1992**, *31*, 2422–2428.
[19] W. R. Harris, C. J. Carrano, K. N. Raymond, *J. Am. Chem. Soc.* **1979**, *101*, 2213–2214.
[20] a) *Handbook of HPLC* (Ed.: D. Corradini), CRC Press, Taylor & Francis, Boca Raton, **2011**; b) D. Kretschy, G. Koellensperger, S. Hann, *Metallomics* **2011**, *3*, 1304–1309.
[21] M. Wacker, A. Seubert, *J. Anal. At. Spectrom.* **2014**, *29*, 707–714.
[22] a) *Handbook of Capillary Electrophoresis Applications* (Ed.: J. Polonski), Chapman & Hall, Springer, London, **1997**; b) C. Allen Chang, C.-Y. Chen, H.-Y. Chen, *J. Chin. Chem. Soc.* **1999**, *46*, 519–528; c) X. Zhu, S. Z. Lever, *Electrophoresis* **2002**, *23*, 1348–1356; d) J. Petit, V. Geertsen, C. Beaucaire, M. Stambouli, *J. Chromatogr. A* **2009**, *1216*, 4113–4120.
[23] M. Pniok, V. Kubicek, J. Havlickova, J. Kotek, A. Sabatie-Gogova, J. Plutnar, S. Huclier-Markai, P. Hermann, *Chem. Eur. J.* **2014**, *20*, 7944–7955.
[24] M. Koudelkova, H. Vinsova, V. Jedinakova-Krizova, *J. Chromatogr. A* **2003**, *990*, 311–316.
[25] C. J. Broan, J. P. L. Cox, A. S. Craig, R. Kataky, D. Parker, A. Harrison, A. M. Randall, G. Ferguson, *J. Chem. Soc., Perkin Trans. 2* **1991**, 87–99.
[26] W. P. Cacheris, S. K. Nickle, A. D. Sherry, *Inorg. Chem.* **1987**, *26*, 958–960.
[27] J. Moreau, E. Guillon, J. C. Pierrard, J. Rimbault, M. Port, M. Aplincourt, *Chem. Eur. J.* **2004**, *10*, 5218–5232.
[28] V. Kubicek, J. Havlickova, J. Kotek, G. Tircso, P. Hermann, E. Toth, I. Lukes, *Inorg. Chem.* **2010**, *49*, 10960–10969.
[29] E. T. Clarke, A. E. Martell, *Inorg. Chim. Acta* **1991**, *190*, 37–46.
[30] R. Garcia, V. Kubíček, B. Drahoš, L. Gano, I. C. Santos, P. Campello, A. Paulo, É. Tóth, I. Santos, *Metallomics* **2010**, *2*, 571–580.
[31] K. Kumar, C. A. Chang, L. C. Francesconi, D. D. Dischino, M. F. Malley, J. Z. Gougoutas, M. F. Tweedle, *Inorg. Chem.* **1994**, *33*, 3567–3575.
[32] R. Pujales-Paradela, A. Rodríguez-Rodríguez, A. Gayoso-Padula, I. Brandariz, L. Valencia, D. Esteban-Gómez, C. Platas-Iglesias, *Dalton Trans.* **2018**, *47*, 13830–13842.
[33] a) A. Roca-Sabio, M. Mato-Iglesias, D. Esteban-Gomez, E. Toth, A. de Blas, C. Platas-Iglesias, T. Rodriguez-Blas, *J. Am. Chem. Soc.* **2009**, *131*, 3331–3341; b) N. A. Thiele, J. J. Woods, J. J. Wilson, *Inorg. Chem.* **2019**, *58*, 10483–10500.
[34] S. Gündüz, S. Vibhute, R. Botár, F. K. Kálmán, I. Tóth, G. Tircsó, M. Regueiro-Figueroa, D. Esteban-Gómez, C. Platas-Iglesias, G. Angelovski, *Inorg. Chem.* **2018**, *57*, 5973–5986.
[35] a) M. Le Fur, M. Beyler, E. Molnár, O. Fougère, D. Esteban-Gómez, G. Tircsó, C. Platas-Iglesias, N. Lepareur, O. Rousseaux, R. Tripier, *Inorg. Chem.* **2018**, *57*, 2051–2063; b) M. Le Fur, E. Molnár, M. Beyler, O. Fougère, D. Esteban-Gómez, O. Rousseaux, R. Tripier, G. Tircsó, C. Platas-Iglesias, *Inorg. Chem.* **2018**, *57*, 6932–6945.
[36] M. Försterová, I. Svobodová, P. Lubal, P. Táborský, J. Kotek, P. Hermann, I. Lukeš, *Dalton Trans.* **2007**, 535–549.
[37] É. Tóth, R. Király, J. Platzek, B. Radüchel, E. Brücher, *Inorg. Chim. Acta* **1996**, *249*, 191–199.
[38] E. Balogh, R. Tripier, P. Fousková, F. Reviriego, H. Handel, É. Tóth, *Dalton Trans.* **2007**, 3572–3581.
[39] Margerum D. W., Cayley G. R., Weatherburn D. C., G. K. Pagenkopf in *Coordination Chemistry, Vol. 2* (Ed.: A. E. Martell), American Chemical Society, Washington, DC, **1978**, pp. 1–220.
[40] a) F. X. Hanin, S. Pauwels, A. Bol, W. Breeman, M. de Jong, F. Jamar, *Nucl. Med. Biol.* **2010**, *37*, 157–165; b) I. Velikyan, H. Maecke, B. Langstrom, *Bioconjugate Chem.* **2008**, *19*, 569–573; c) I. Velikyan, G. J. Beyer, E. Bergstrom-Pettermann, P. Johansen, M. Bergstrom, B. Langstrom, *Nucl. Med. Biol.* **2008**, *35*, 529–536; d) L. M. De Leon-Rodriguez, Z. Kovacs, *Bioconjugate Chem.* **2008**, *19*, 391–402; e) M. S. Cooper, E. Sabbah, S. J. Mather, *Nat. Protoc.* **2006**, *1*, 314–317; f) T. W. Price, J. Greenman, G. J. Stasiuk, *Dalton Trans.* **2016**, *45*, 15702–15724.
[41] J. F. Desreux, *Inorg. Chem.* **1980**, *19*, 1319–1324.
[42] E. Brücher, G. Laurenczy, Z. S. Makra, *Inorg. Chim. Acta* **1987**, *139*, 141–142.
[43] a) P. Taborsky, I. Svobodova, P. Lubal, Z. Hnatejko, S. Lis, P. Hermann, *Polyhedron* **2007**, *26*, 4119–4130; b) S. L. Wu, W. D. Horrocks, *Inorg. Chem.* **1995**, *34*, 3724–3732.
[44] a) E. Balogh, R. Tripier, R. Ruloff, E. Toth, *Dalton Trans.* **2005**, 1058–1065; b) E. Szilagyi, E. Toth, Z. Kovacs, J. Platzek, B. Raduchel, E. Brucher, *Inorg. Chim. Acta* **2000**, *298*, 226–234; c) P. Taborsky, P. Lubal, J. Havel, J. Kotek, P. Hermann, I. Lukes, *Collect. Czech. Chem. Commun.* **2005**, *70*, 1909–1942.
[45] S. P. Kasprzyk, R. G. Wilkins, *Inorg. Chem.* **1982**, *21*, 3349–3352.
[46] K. Kumar, M. F. Tweedle, *Inorg. Chem.* **1993**, *32*, 4193–4199.
[47] S. Procházková, J. Hraníček, V. Kubíček, P. Hermann, *Polyhedron* **2016**, *111*, 143–149.
[48] G. Tircso, Z. Kovacs, A. D. Sherry, *Inorg. Chem.* **2006**, *45*, 9269–9280.
[49] G. Tircso, E. T. Benyo, E. H. Suh, P. Jurek, G. E. Kiefer, A. D. Sherry, Z. Kovacs, *Bioconjugate Chem.* **2009**, *20*, 565–575.
[50] F. K. Kalman, Z. Baranyai, I. Toth, I. Banyai, R. Kiraly, E. Brucher, S. Aime, X. Sun, A. D. Sherry, Z. Kovacs, *Inorg. Chem.* **2008**, *47*, 3851–3862.
[51] F. K. Kalman, Thesis, University of Debrecen, **2007**.
[52] L. Burai, R. Kiraly, I. Lazar, E. Brucher, *Eur. J. Inorg. Chem.* **2001**, *2001*, 813–820.
[53] L. Tei, Z. Baranyai, L. Gaino, A. Forgacs, A. Vagner, M. Botta, *Dalton Trans.* **2015**, *44*, 5467–5478.
[54] S. Aime, M. Botta, Z. Garda, B. E. Kucera, G. Tircso, V. G. Young, M. Woods, *Inorg. Chem.* **2011**, *50*, 7955–7965.
[55] E. Eppard, M. Pèrez-Malo, F. Rösch, *EJNMMI Radiopharm. Chem.* **2016**, *1*, 6–19.
[56] J. C. Bunzli, *Chem. Rev.* **2010**, *110*, 2729–2755.
[57] Z. Baranyai, Z. Pálinkás, F. Uggeri, A. Maiocchi, S. Aime, E. Brücher, *Chem. Eur. J.* **2012**, *18*, 16426–16435.
[58] E. Szilagyi, E. Toth, E. Brucher, A. E. Merbach, *J. Chem. Soc., Dalton Trans.* **1999**, 2481–2486.
[59] a) H.-Z. Cai, T. A. Kaden, *Helv. Chim. Acta* **1994**, *77*, 383–398; b) S. Laurent, L. V. Elst, F. Copoix, R. N. Muller, *Invest. Radiol.* **2001**, *36*, 115–122.
[60] K. Kumar, C. A. Chang, M. F. Tweedle, *Inorg. Chem.* **1993**, *32*, 587–593.
[61] C. A. Chang, Y.-L. Liu, *J. Chin. Chem. Soc.* **2000**, *47*, 1001–1006.
[62] W. Schwizer, R. Fraser, H. Maecke, K. Siebold, R. Funck, M. Fried, *Magn. Reson. Med.* **1994**, *31*, 388–393.
[63] M. P. Campello, S. Lacerda, I. C. Santos, G. A. Pereira, C. F. Geraldes, J. Kotek, P. Hermann, J. Vanek, P. Lubal, V. Kubicek, E. Toth, I. Santos, *Chem. Eur. J.* **2010**, *16*, 8446–8465.
[64] M. P. Campello, M. Balbina, I. Santos, P. Lubal, R. Ševčík, R. Ševčíková, *Helv. Chim. Acta* **2009**, *92*, 2398–2413.
[65] M. Woods, Z. Kovacs, R. Kiraly, E. Brucher, S. Zhang, A. D. Sherry, *Inorg. Chem.* **2004**, *43*, 2845–2851.
[66] T. J. Norman, D. Parker, L. Royle, A. Harrison, P. Antoniw, D. J. King, *J. Chem. Soc., Chem. Commun.* **1995**, 1877–1878.
[67] K. P. Pulukkody, T. J. Norman, D. Parker, L. Royle, C. J. Broan, *J. Chem. Soc., Perkin Trans. 2* **1993**, 605–620.
[68] C. F. Baes, R. E. Mesmer, *The Hydrolysis of Cations*, John Wiley & Son, New York, London, Sydney, Toronto, **1976**.
[69] H. Stetter, W. Frank, *Angew. Chem. Int. Ed. Engl.* **1976**, *15*, 686–686; *Angew. Chem.* **1976**, *88*, 760.
[70] C. C. Bryden, C. N. Reilley, J. F. Desreux, *Anal. Chem.* **1981**, *53*, 1418–1425.
[71] M. R. Spirlet, J. Rebizant, M. F. Loncin, J. F. Desreux, *Inorg. Chem.* **1984**, *23*, 4278–4283.
[72] a) M. Magerstadt, O. A. Gansow, M. W. Brechbiel, D. Colcher, L. Baltzer, R. H. Knop, M. E. Girton, M. Naegele, *Magn. Reson. Med.* **1986**, *3*, 808–812; b) J. N. Caille, P. Kien, M. Allard, B. Bonnemain, *Am. J. Neuroradiol.* **1986**, *7*, 540–540.
[73] R. B. Lauffer, *Chem. Rev.* **1987**, *87*, 901–927.
[74] a) D. D. Dischino, E. J. Delaney, J. E. Emswiler, G. T. Gaughan, J. S. Prasad, S. K. Srivastava, M. F. Tweedle, *Inorg. Chem.* **1991**, *30*, 1265–1269; b) K. Kumar, T. Jin, X. Wang, J. F. Desreux, M. F. Tweedle, *Inorg. Chem.* **1994**, *33*, 3823–3829.
[75] a) H. Vogler, J. Platzek, G. Schuhmann-Giampieri, T. Frenzel, H. J. Weinmann, B. Raduchel, W. R. Press, *Eur. J. Radiol.* **1995**, *21*, 1–10; b) T. Staks,

G. Schuhmann-Giampieri, T. Frenzel, H. J. Weinmann, L. Lange, J. Platzek, *Invest. Radiol.* **1994**, *29*, 709–715.

[76] S. Aime, M. Botta, E. Terreno in *Gd(III)-BASED CONTRAST AGENTS FOR MRI* in *Adv. Inorganic Chemistry*, *Vol. 57* Academic Press, **2005**, pp. 173–237.

[77] a) P. Caravan, J. J. Ellison, T. J. McMurry, R. B. Lauffer, *Chem. Rev.* **1999**, *99*, 2293–2352; b) T. J. Clough, L. Jiang, K.-L. Wong, N. J. Long, *Nat. Commun.* **2019**, *10*, 1420–1433; c) J. Wahsner, E. M. Gale, A. Rodríguez-Rodríguez, P. Caravan, *Chem. Rev.* **2019**, *119*, 957–1057.

[78] S. Aime, Z. Baranyai, E. Gianolio, E. Terreno in *Paramagnetic Contrast Agents*, *Vol.* Eds.: M. Modo, J. Bulte), CRC Press, Boca Raton, **2007**.

[79] V. C. Pierre, M. J. Allen, *Contrast Agents for MRI: Experimental Methods* Royal Society of Chemistry (RCS), Cambridge, **2018**, p.

[80] a) S. Aime, E. Gianolio, E. Terreno, G. B. Giovenzana, R. Pagliarin, M. Sisti, G. Palmisano, M. Botta, M. P. Lowe, D. Parker, *J. Biol. Inorg. Chem.* **2000**, *5*, 488–497; b) S. Aime, M. Botta, L. Frullano, S. Geninatti Crich, G. Giovenzana, R. Pagliarin, G. Palmisano, F. R. Sirtori, M. Sisti, *J. Med. Chem.* **2000**, *43*, 4017–4024.

[81] a) D. A. Fulton, M. O'Halloran, D. Parker, K. Senanayake, M. Botta, S. Aime, *Chem. Commun.* **2005**, 474–476; b) L. Vander Elst, M. Port, I. Raynal, C. Simonot, R. N. Muller, *Eur. J. Inorg. Chem.* **2003**, *2003*, 2495–2501; c) L. Vander Elst, I. Raynal, M. Port, P. Tisnès, R. N. Muller, *Eur. J. Inorg. Chem.* **2005**, *2005*, 1142–1148.

[82] S. Aime, M. Botta, E. Terreno, P. L. Anelli, F. Uggeri, *Magn. Reson. Med.* **1993**, *30*, 583–591.

[83] a) E. Boros, P. Caravan, *J. Med. Chem.* **2013**, *56*, 1782–1786; b) S. Aime, E. Gianolio, D. Longo, R. Pagliarin, C. Lovazzano, M. Sisti, *ChemBioChem* **2005**, *6*, 818–820.

[84] K. Overoye-Chan, S. Koerner, R. J. Looby, A. F. Kolodziej, S. G. Zech, Q. Deng, J. M. Chasse, T. J. McMurry, P. Caravan, *J. Am. Chem. Soc.* **2008**, *130*, 6025–6039.

[85] C. T. Farrar, E. M. Gale, R. Kennan, I. Ramsay, R. Masia, G. Arora, K. Looby, L. Wei, J. Kalpathy-Cramer, M. M. Bunzel, C. Zhang, Y. Zhu, T. E. Akiyama, M. Klimas, S. Pinto, H. Diyabalanage, K. K. Tanabe, V. Humblet, B. C. Fuchs, P. Caravan, *Radiology* **2018**, *287*, 581–589.

[86] A. F. Martins, D. M. Dias, J.-F. Morfin, S. Lacerda, D. V. Laurents, É. Tóth, C. F. G. C. Geraldes, *Chem. Eur. J.* **2015**, *21*, 5413–5422.

[87] Y.-S. Kim, Y. Zhou, H. Bryant, D. E. Milenic, K. E. Baidoo, B. K. Lewis, J. A. Frank, M. W. Brechbiel, *Bioorg. Med. Chem. Lett.* **2015**, *25*, 2056–2059.

[88] T. L. Kalber, N. Kamaly, P.-W. So, J. A. Pugh, J. Bunch, C. W. McLeod, M. R. Jorgensen, A. D. Miller, J. D. Bell, *Mol. Imag. Biol.* **2011**, *13*, 653–662.

[89] H. Kobayashi, M. W. Brechbiel, *Curr. Pharm. Biotechnol.* **2004**, *5*, 539–549.

[90] W. J. Mulder, G. J. Strijkers, G. A. van Tilborg, D. P. Cormode, Z. A. Fayad, K. Nicolay, *Acc. Chem. Res.* **2009**, *42*, 904–914.

[91] a) S. Aime, D. Delli Castelli, E. Terreno, *Angew. Chem. Int. Ed.* **2002**, *41*, 4334–4336; *Angew. Chem.* **2002**, *114*, 4510; b) Z. Baranyai, G. A. Rolla, R. Negri, A. Forgacs, G. B. Giovenzana, L. Tei, *Chem. Eur. J.* **2014**, *20*, 2933–2944.

[92] S. Aime, M. Botta, E. Gianolio, E. Terreno, *Angew. Chem. Int. Ed.* **2000**, *39*, 747–750; *Angew. Chem.* **2000**, *112*, 763.

[93] S. Zhang, R. Trokowski, A. D. Sherry, *J. Am. Chem. Soc.* **2003**, *125*, 15288–15289.

[94] a) E. L. Que, C. J. Chang, *Chem. Soc. Rev.* **2010**, *39*, 51–60; b) A. C. Esqueda, J. A. López, G. Andreu-de-Riquer, J. C. Alvarado-Monzón, J. Ratnakar, A. J. M. Lubag, A. D. Sherry, L. M. De León-Rodríguez, *J. Am. Chem. Soc.* **2009**, *131*, 11387–11391; c) W.-h. Li, S. E. Fraser, T. J. Meade, *J. Am. Chem. Soc.* **1999**, *121*, 1413–1414; d) F. Garello, S. Vibhute, S. Gündüz, N. K. Logothetis, E. Terreno, G. Angelovski, *Biomacromolecules* **2016**, *17*, 1303–1311.

[95] C. Carrera, G. Digilio, S. Baroni, D. Burgio, S. Consol, F. Fedeli, D. Longo, A. Mortillaro, S. Aime, *Dalton Trans.* **2007**, 4980–4987.

[96] a) B. Yoo, M. D. Pagel, *J. Am. Chem. Soc.* **2006**, *128*, 14032–14033; b) R. Napolitano, G. Pariani, F. Fedeli, Z. Baranyai, M. Aswendt, S. Aime, E. Gianolio, *J. Med. Chem.* **2013**, *56*, 2466–2477.

[97] S. Achilefu, *Chem. Rev.* **2010**, *110*, 2575–2578.

[98] M. Meckel, V. Kubicek, P. Hermann, M. Miederer, F. Rosch, *Nucl. Med. Biol.* **2016**, *43*, 670–678.

[99] a) K. P. Eisenwiener, M. I. Prata, I. Buschmann, H. W. Zhang, A. C. Santos, S. Wenger, J. C. Reubi, H. R. Macke, *Bioconjugate Chem.* **2002**, *13*, 530–541; b) J. Notni, P. Hermann, J. Havlickova, J. Kotek, V. Kubicek, J. Plutnar, N. Loktionova, P. J. Riss, F. Rosch, I. Lukes, *Chem. Eur. J.* **2010**, *16*, 7174–7185; c) E. T. Clarke, A. E. Martell, *Inorg. Chim. Acta* **1991**, *190*, 27–36.

[100] a) M. T. Ma, C. Cullinane, C. Imberti, J. Baguna Torres, S. Y. Terry, P. Roselt, R. J. Hicks, P. J. Blower, *Bioconjugate Chem.* **2016**, *27*, 309–318; b) M. S. Hofman, P. Eu, P. Jackson, E. Hong, D. Binns, A. Iravani, D. Murphy, C. Mitchell, S. Siva, R. J. Hicks, J. D. Young, P. J. Blower, G. E. Mullen, *J. Nucl. Med.* **2018**, *59*, 625–631.

[101] a) G. Nagy, D. Szikra, G. Trencsenyi, A. Fekete, I. Garai, A. M. Giani, R. Negri, N. Masciocchi, A. Maiocchi, F. Uggeri, I. Toth, S. Aime, G. B. Giovenzana, Z. Baranyai, *Angew. Chem. Int. Ed.* **2017**, *56*, 2118–2122; *Angew. Chem.* **2017**, *129*, 2150; b) L. Manzoni, L. Belvisi, D. Arosio, M. P. Bartolomeo, A. Bianchi, C. Brioschi, F. Buonsanti, C. Cabella, C. Casagrande, M. Civera, M. De Matteo, L. Fugazza, L. Lattuada, F. Maisano, L. Miragoli, C. Neira, M. Pilkington-Miksa, C. Scolastico, *ChemMedChem* **2012**, *7*, 1084–1093; c) J. P. Sinnes, J. Nagel, B. P. Waldron, T. Maina, A. Nock, R. Bergmann, M. Ullrich, J. Pietzsch, M. Bachmann, R. P. Baum, F. Rösch, *EJNMMI Res.* **2019**, *9*, 48; d) J. Seemann, B. P. Waldron, F. Roesch, D. Parker, *ChemMedChem* **2015**, *10*, 1019–1026.

[102] M. de Jong, W. H. Bakker, E. P. Krenning, W. A. Breeman, M. E. van der Pluijm, B. F. Bernard, T. J. Visser, E. Jermann, M. Behe, P. Powell, H. R. Macke, *Eur. J. Nucl. Med.* **1997**, *24*, 368–371.

[103] a) F. Rösch, H. Herzog, S. Qaim, *Pharmaceuticals* **2017**, *10*, 56; b) F. Jamar, R. Barone, I. Mathieu, S. Walrand, D. Labar, P. Carlier, J. de Camps, H. Schran, T. Chen, M. C. Smith, H. Bouterfa, R. Valkema, E. P. Krenning, L. K. Kvols, S. Pauwels, *Eur. J. Nucl. Med. Mol. Imaging* **2003**, *30*, 510–518.

[104] a) K. P. Zhernosekov, D. V. Filosofov, R. P. Baum, P. Aschoff, H. Bihl, A. A. Razbash, M. Jahn, M. Jennewein, F. Rosch, *J. Nucl. Med.* **2007**, *48*, 1741–1748; b) S. Koukouraki, L. G. Strauss, V. Georgoulias, J. Schuhmacher, U. Haberkorn, N. Karkavitsas, A. Dimitrakopoulou-Strauss, *Eur. J. Nucl. Med. Mol. Imaging* **2006**, *33*, 460–466.

[105] a) M. Hofmann, H. Maecke, R. Borner, E. Weckesser, P. Schoffski, L. Oei, J. Schumacher, M. Henze, A. Heppeler, J. Meyer, H. Knapp, *Eur. J. Nucl. Med.* **2001**, *28*, 1751–1757; b) G.-J. Meyer, H. Mäcke, J. Schuhmacher, W. H. Knapp, M. Hofmann, *Eur. J. Nucl. Med. Mol. Imaging* **2004**, *31*, 1097–1104.

[106] a) C. Kratochwil, F. L. Giesel, F. Bruchertseifer, W. Mier, C. Apostolidis, R. Boll, K. Murphy, U. Haberkorn, A. Morgenstern, *Eur. J. Nucl. Med. Mol. Imaging* **2014**, *41*, 2106–2119; b) F. Rösch, R. P. Baum, *Dalton Trans.* **2011**, *40*, 6104–6111; c) A. Singh, N. P. van der Meulen, C. Muller, I. Klette, H. R. Kulkarni, A. Turler, R. Schibli, R. P. Baum, *Cancer Biother. Radiopharm.* **2017**, *32*, 124–132; d) R. P. Baum, A. Singh, M. Benešová, C. Vermeulen, S. Gnesin, U. Köster, K. Johnston, D. Müller, S. Senftleben, H. R. Kulkarni, A. Türler, R. Schibli, J. O. Prior, N. P. van der Meulen, C. Müller, *Dalton Trans.* **2017**, *46*, 14638–14646.

[107] M. Benesova, M. Schafer, U. Bauder-Wust, A. Afshar-Oromieh, C. Kratochwil, W. Mier, U. Haberkorn, K. Kopka, M. Eder, *J. Nucl. Med.* **2015**, *56*, 914–920.

[108] a) C. Kratochwil, F. L. Giesel, M. Eder, A. Afshar-Oromieh, M. Benesova, W. Mier, K. Kopka, U. Haberkorn, *Eur. J. Nucl. Med. Mol. Imaging* **2015**, *42*, 987–988; b) A. Delker, W. P. Fendler, C. Kratochwil, A. Brunegraf, A. Gosewisch, F. J. Gildehaus, S. Tritschler, C. G. Stief, K. Kopka, U. Haberkorn, P. Bartenstein, G. Boning, *Eur. J. Nucl. Med. Mol. Imaging* **2016**, *43*, 42–51; c) H. Rathke, P. Flechsig, W. Mier, M. Bronzel, E. Mavriopoulou, M. Roehrich, M. Hohenfellner, F. L. Giesel, U. L. Haberkorn, C. Kratochwil, *J. Nucl. Med.* **2019**, *60*, 806–811; d) C. Kratochwil, K. Schmidt, A. Afshar-Oromieh, F. Bruchertseifer, H. Rathke, A. Morgenstern, U. Haberkorn, F. L. Giesel, *Eur. J. Nucl. Med. Mol. Imaging* **2018**, *45*, 31–37; e) C. Kratochwil, F. Bruchertseifer, F. L. Giesel, M. Weis, F. A. Verburg, F. Mottaghy, K. Kopka, C. Apostolidis, U. Haberkorn, A. Morgenstern, *J. Nucl. Med.* **2016**, *57*, 1941–1944.

[109] a) A. Khawar, E. Eppard, J. P. Sinnes, F. Roesch, H. Ahmadzadehfar, S. Kurpig, M. Meisenheimer, F. C. Gaertner, M. Essler, R. A. Bundschuh, *Clin. Nucl. Med.* **2018**, *43*, 486–491; b) E. Eppard, A. de la Fuente, M. Benesova, A. Khawar, R. A. Bundschuh, F. C. Gartner, B. Kreppel, K. Kopka, M. Essler, F. Rosch, *Theranostics* **2017**, *7*, 4359–4369.

[110] a) T. Maina, B. A. Nock, H. Kulkarni, A. Singh, R. P. Baum, *PET Clin.* **2017**, *12*, 297–309; b) B. A. Nock, A. Kaloudi, E. Lymperis, A. Giarika, H. R. Kulkarni, I. Klette, A. Singh, E. P. Krenning, M. de Jong, T. Maina, R. P. Baum, *J. Nucl. Med.* **2017**, *58*, 75–80.

[111] a) A. Poschenrieder, M. Schottelius, M. Schwaiger, H. Kessler, H.-J. Wester, *EJNMMI Res.* **2016**, *6*, 36; b) M. Kircher, P. Herhaus, M. Schottelius, A. K. Buck, R. A. Werner, H. J. Wester, U. Keller, C. Lapa, *Ann. Nucl. Med.* **2018**, *32*, 503–511.
[112] a) M. Meckel, R. Bergmann, M. Miederer, F. Roesch, *EJNMMI Radiopharm. Chem.* **2017**, *1*, 14; b) R. Bergmann, M. Meckel, V. Kubicek, J. Pietzsch, J. Steinbach, P. Hermann, F. Rosch, *EJNMMI Res.* **2016**, *6*, 5; c) M. Fellner, B. Biesalski, N. Bausbacher, V. Kubicek, P. Hermann, F. Rosch, O. Thews, *Nucl. Med. Biol.* **2012**, *39*, 993–999; d) N. Pfannkuchen, N. Bausbacher, S. Pektor, M. Miederer, F. Rosch, *Curr. Radiopharm.* **2018**, *11*, 223–230; e) N. Pfannkuchen, M. Meckel, R. Bergmann, M. Bachmann, C. Bal, M. Sathekge, W. Mohnike, R. Baum, F. Rösch, *Pharmaceuticals* **2017**, *10*, 45.
[113] IUPAC. *Compendium of Chemical Terminology*, 2nd ed. (the "Gold Book", compiled by A. D. McNaught, A. Wilkinson), Blackwell Scientific Publications, Oxford, **1997**, p. 2520.
[114] a) H. Matsuura in *Hot Atom Chemistry: Recent trends and applications in the physical and life sciences and technology*, (Ed.: H. Matsuura), Kodansha Ltd., Tokyo, **1984**, pp. 378–382; b) J.-P. Adloff, P. P. Gaspar, M. Imamura, A. G. Maddock, T. Matsuura, H. Sano, K. Yoshihara, *Handbook of hot atom chemistry.*, Kodansha Ltd., VCH, Weinheim, New York, Cambridge, Basel, **1992**.
[115] E. Rutherford, *Radioactivity*, Cambridge University Press, Cambridge, **1904**, p. 392.
[116] W. Lanouette, B. Szilard, *Genius in the shadows: A biography of Leo Szilard.*, Maxwell MacMillan International, New York, Oxford, Singapore, Sydney, **1992**, p.
[117] L. Szilard, T. A. Chalmers, *Nature* **1934**, *134*, 462.
[118] H. Ebihara, K. E. Collins in *Production of radionuclide using hot atom chemistry* (Ed.: H. Matsuura), Kodansha Ltd., Tokyo, **1984**, p. 378.
[119] K. P. Zhernosekov, D. V. Filosofov, F. Rösch, *Radiochim. Acta* **2012**, *100*, 669.
[120] a) E. Segrè, R. S. Halford, G. T. Seaborg, *Phys. Rev.* **1939**, *55*, 321–322; b) T. Stenström, B. Jung, *Radiochim. Acta* **1965**, *4*, 3.
[121] K. P. Zhernosekov, D. V. Filosofov, M. Qaim Syed, F. Rösch, *Radiochim. Acta* **2007**, *95*, 319–327.
[122] T. Moeller, L. C. Thompson, *J. Inorg. Nucl. Chem.* **1962**, *24*, 499–510.
[123] G. Anderegg, *Helv. Chim. Acta* **1960**, *43*, 825–830.
[124] T. V. Beloedova, L. V. Kazakova, N. A. Skorik, *Russ. J. Inorg. Chem.* **1972**, *17*, 1580–1583.
[125] F. Rösch, J. Brockmann, N. A. Lebedev, S. M. Qaim, *Acta Oncologica* **2000**, *39*, 727–730.
[126] F. Rösch in *Nuclear- and Radiochemistry*, *Vol. 2* Walter de Gruyter, Berlin/Boston, **2014**.
[127] R. Bhardwaj, A. van der Meer, S. K. Das, M. de Bruin, J. Gascon, H. T. Wolterbeek, A. G. Denkova, P. Serra-Crespo, *Sci. Rep.* **2017**, *7*, 44242.
[128] S. Huclier-Markai, R. Kerdjoudj, C. Alliot, A. C. Bonraisin, N. Michel, F. Haddad, J. Barbet, *Nucl. Med. Biol.* **2014**, *41*, e36–43.
[129] a) F. Rösch, F. F. Knapp in *Radionuclide Generators*, *Vol. 4* (Eds.: A. Vértes, S. Nagy, Z. Klencsár, R. G. Lovas, F. Rösch), Springer, Berlin-Heidelberg, **2011**, pp. 1935–1976; b) P. E. Edem, J. Fonslet, A. Kjær, M. Herth, G. Severin, *Bioinorg. Chem. Appl.* **2016**, *2016*, 8; c) N. Trautmann, F. Rösch in *Radiochemical Separations*, *Vol. II: Modern Applications* (Ed.: F. Rösch), Walter de Gruyter, Berlin, Boston, **2016**, pp. 215–254; d) J. R. Zeevaart, Z. Szucs, S. Takacs, J. van Rooyen, D. Jansen, *J. Labelled Compd. Radiopharm.* **2012**, *55*, 115–119.
[130] N. A. Lebedev, A. F. Novgorodov, R. Misiak, J. Brockmann, F. Rosch, *Appl. Radiat. Isot.* **2000**, *53*, 421–425.
[131] a) F. G. Kondev, *Nucl. Data Sheets* **2003**, *98*, 801–1095; b) F. G. Kondev, I. Ahmad, M. P. Carpenter, J. P. Greene, R. V. F. Janssens, T. Lauritsen, D. Seweryniak, S. Zhu, S. P. Lalkovski, P. Chowdhury, *Appl. Radiat. Isot.* **2012**, *70*, 1867–1870.
[132] a) D. V. Filosofov, N. S. Loktionova, F. Rösch, *Radiochim. Acta* **2010**, *98*, 149–156; b) M. Pruszynski, N. S. Loktionova, D. V. Filosofov, F. Rosch, *Appl. Radiat. Isot.* **2010**, *68*, 1636–1641; c) F. Roesch, *Curr. Radiopharmaceuticals* **2012**, *5*, 187–201.
[133] G. W. Severin, J. W. Engle, H. F. Valdovinos, T. E. Barnhart, R. J. Nickles, *Appl. Radiat. Isot.* **2012**, *70*, 1526–1530.
[134] G. Severin, M. Munch, M. Jensen, *J. Labelled Compd. Radiopharm.* **2013**, *56*, S220.
[135] G. W. Severin, L. K. Kristensen, C. H. Nielsen, J. Fonslet, A. I. Jensen, A. F. Frellsen, K. M. Jensen, D. R. Elema, H. Maecke, A. Kjaer, K. Johnston, U. Koster, *Front. Med.* **2017**, *4*, 98.

Received: June 29, 2019